Mechanical Design of De-Dusting System for Sinter Plant

By

Ravi Prakash

13MMED11

DEPARTMENT OF MECHANICAL ENGINEERING
INSTITUTE OF TECHNOLOGY
NIRMA UNIVERSITY

AHMEDABAD-382481

MAY 2015

Mechanical Design of De-Dusting System for Sinter Plant

Major Project Report

Submitted in partial fulfillment of the requirements

For the Degree of

Master of Technology in Mechanical Engineering (Design Engineering)

By

Ravi Prakash

(13MMED11)

Guided By

Prof. D.B Shah

DEPARTMENT OF MECHANICAL ENGINEERING

INSTITUTE OF TECHNOLOGY
NIRMA UNIVERSITY

AHMEDABAD-382 481

MAY 2015

Declaration

This is to certify that

1. The thesis comprises my original work towards the degree of Master of Technology in Design Engineering at Nirma University and has not been submitted elsewhere for a degree or diploma.

2. Due acknowledgement has been made in the text to all other material used.

Ravi Prakash

13MMED11

Undertaking for Originality of the Work

I, Ravi Prakash, Roll. No. 13MMED11, give undertaking that the Major Project entitled "Mechanical Design of De-Dusting System for Sinter Plant" submitted by me, towards the partial fulfillment of the requirements for the degree of Master of Technology in Mechanical Engineering (Design) of Nirma University, Ahmedabad, is the original work carried out by me and I give assurance that no attempt of plagiarism has been made. I understand that in the event of any similarity found subsequently with any published work or any dissertation work elsewhere; it will result in severe disciplinary action.

_____

Signature of Student

Date: _____

Place: Nirma University,Ahmedabad

Endorsed By

(Signature of Institute Guide)

Certificate

This is to certify that the Major Project Report entitled **"Mechanical Design of De-Dusting System for Sinter Plant"** submitted by **Ravi Prakash (13MMED11)**, towards the partial fulfillment of the requirements for the award of Degree of **Master of Technology in Mechanical Engineering (Design Engineering)** of Institute of Technology, Nirma University, Ahmadabad is the record of work carried out by him under our supervision and guidance. In our opinion, the submitted work has reached a level required for being accepted for examination.The result embodied in this major project, to the best of our knowledge, has not been submitted to any other University or Institution for award of any degree.

Mr. D.B Shah
Assistant Professor and Guide
Department of Mechanical Engineering,
Institute of Technology, Nirma University,
Ahmedabad.

Dr. R. N. Patel
Professor and Head,
Department of Mechanical Engineering,
Institute of Technology,
Nirma University,
Ahmedabad.

Dr K Kotecha
Director,
Institute of Technology,
Nirma University,
Ahmedabad.

Acknowledgments

I express deep gratitude to thank my institute project guide **Prof. D.B Shah** and industry project guide **Mr. Janmesh Pandya** for helping me with the conceptualization of the idea for the project, providing the technical assistance and prompt suggestions from him during my thesis work. I candidly thank **Prof. D.B Shah** and **Mr. Janmesh Pandya** for giving me motivation whenever required and standing beside me throughout the journey.

I would like to thank **Dr. R.N Patel** Head of Mechanical Engineering Department, for having faith in me and supporting me throughout my endeavor.

I express deep gratitude to **Dr K Kotecha** (Director, ITNU) and all teaching and non-teaching staff of mechanical engineering department who had helped me knowingly or unknowingly and for having instilled in me.

I would also like to thank god, my parents and all my friends who have help me and for the moral support throughout the dissertation. I remain highly grateful to them and it is my earnest desire to acknowledge all of them

Ravi Prakash

Abstract

In sinter plant a lot of dust is generated during sintering process, which cause harmful effect on health of workers, air pollution and also reduce the visibility of working environment. Therefore, de-dusting system is required to extracts the dust laden air from working site and made the working environment clean. De-dusting system have duct network, cyclonic separator, and stack as its main components.

Duct network is very critical component to maintain desired amount of flow, which is achieved by maintaining nearly same pressure drop inside duct network. The duct network of de-dusting system is subjected to external pressure or load, so required special attention during designing regarding selection of appropriate code, material, etc. ASME BPV section VIII division I is used to design duct subject to external pressure. The result of pressure balancing and thickness selection for pipes is validated using PIPENET and PV Elite software respectively. Cyclonic separator, which ensure collection of dust particle from the dust laden air so, design and installation of cyclonic separator is necessary. Different methods is used to design and selection of best model for cyclonic separator which suited to given criteria. The velocity at different points and pressure drop is validated through ANSYS CFX. Steel stack, is tall and lightly damped structures with circular cross-sections subjected to wind-exited vibration. The geometry of a self supporting steel stack plays a vital role because of stiffness parameter in structural behavior under lateral dynamic loading. However the basic dimensions of industrial self supporting steel stack, such as height, diameter at exit, etc., are generally derived from the associated environmental conditions. The IS-6533: 1989 Part 1 and 2 code is used to ensure a safe working design of self supporting stack.

Contents

List of Figures

List of Tables

Nomenclature

Variables	Physical Quantity	Unit
A	Constant	
a	Inlet height	m
B	Constant	
b	Inlet width	m
C	Local loss coefficient/ Dynamic loss	MPa
D	Diameter	mm
D_o	Outer diameter	mm
D_i	Inner diameter	mm
$[d_p]_{cut}$	Cut diameter	µm
$d_{p50\%}$	Cut dia. for 50% collection efficiency	µm
E	Young's modulus	MPa
f	Darcy friction factor	
g	Acceleration due to gravity	m/s^2
h	Height of cylindrical portion	m
H	Total height	m
I	Moment of inertia	m^4
K	Configuration factor	
K_1	Risk factor	
K_2	Size factor	
K_3	Topological factor	
n_t	Number of turns	
n	Vortex exponent	
L	Length	m
P_v	Velocity pressure	$kg - s/m^2$
$\triangle P_f$	Friction loss	Pa
Q	Flow rate	m^3/s
s	Length of inside cylinder	m
T_n	Natural period of vibration	s
T	Fundamental period of vibration	s
t	Thickness	mm
U	Mean wind speed	m/s
V	Velocity of dust-laden air	m/s
V_b	Basic wind velocity	m/s
V_z	Design wind speed	m/s

Variables	Physical Quantity	Unit
W	Weight	kg
y	Deflection	mm
Z	Section modulus	m^3
Re	Reynolds number	

Subscripts	
a	Air
allow	Allowable
b	Branch
c	Compressive
den	Denominator
g	Gas
h	Horizontal
o	Outer
i	Inner
num	Numerator
m	Material
mo	Bending
pl	Platform
ref	Refer
t	Top
ln	Logarithmic mean
s	Main duct
sh	Shear
1,2,3 and 4	Parts

Greek		
ε	Roughness factor	mm
$\triangle$	Difference	
ρ	Density	kg/m^3
μ	Dynamic viscosity	Ns/m^3
ν	Kinematic viscosity	m^2/s
η	Collection efficiency	%
η_o	Overall efficiency	%

Acronyms	
ACI	American Concrete Institute
AED	Aerodynamic Equivalent Diameter
ASHRAE	American Society of Heating,Refrigeration and Air Conditioning Engineers
ASME	American Society Of Mechanical Engineers
ESD	Equivalent Spherical Diameter
PM	Particulate matter
PSD	Particle size Distribution

Chapter 1

Introduction

Today whole world is suffers from one of the major problem which is air pollution. This causes health related problem as well as degrade the environment. Due to this Government shows special concern and makes strict rules and regulation to restrict the pollution and also set strict norms and condition for the industries for proper and safely emission of flue. The main objective of this dissertation is to following the norms of Government and mechanically design different component of de-dusting system for sinter plant. So that a safer and clean working environment is provided to peoples along with protecting the environment from adverse effect of pollution.

1.1 Description of de-dusting system for sinter plant

Steel making industry uses iron ore generally magnetite for extraction of iron, for making billets, plates with variable thickness, coil etc.Iron ore as in its raw form cannot be used therefore it is needed to reduce the iron ore to some reducible form which can be directly used in furnace for extraction of iron. So the process of converting iron ore into reducible form is known as sintering and the plant is called sinter plant. During the process the iron ore in powder form moves from one conveyor to another from grinding section to screening section through mixing and balling section. So, dropping of powder form of iron ore from one conveyor belt to another and during further sintering process, the dust releases.The flow diagram of sinter plant is shown in fig. 1.1

As these dust laden air not only degrade the working environment of industry but also have adverse effect to workers health and cause air pollution. To restrict the air pollution the Government makes various strict rules and regulation for industry. So there is a need to install de-dusting system for sinter plant.The site is selected from where the dust is arises.This sites are generally the point on the conveyor from which powder iron ore falls. And that site a hood is mounted for for extraction of dusty air from working environment.

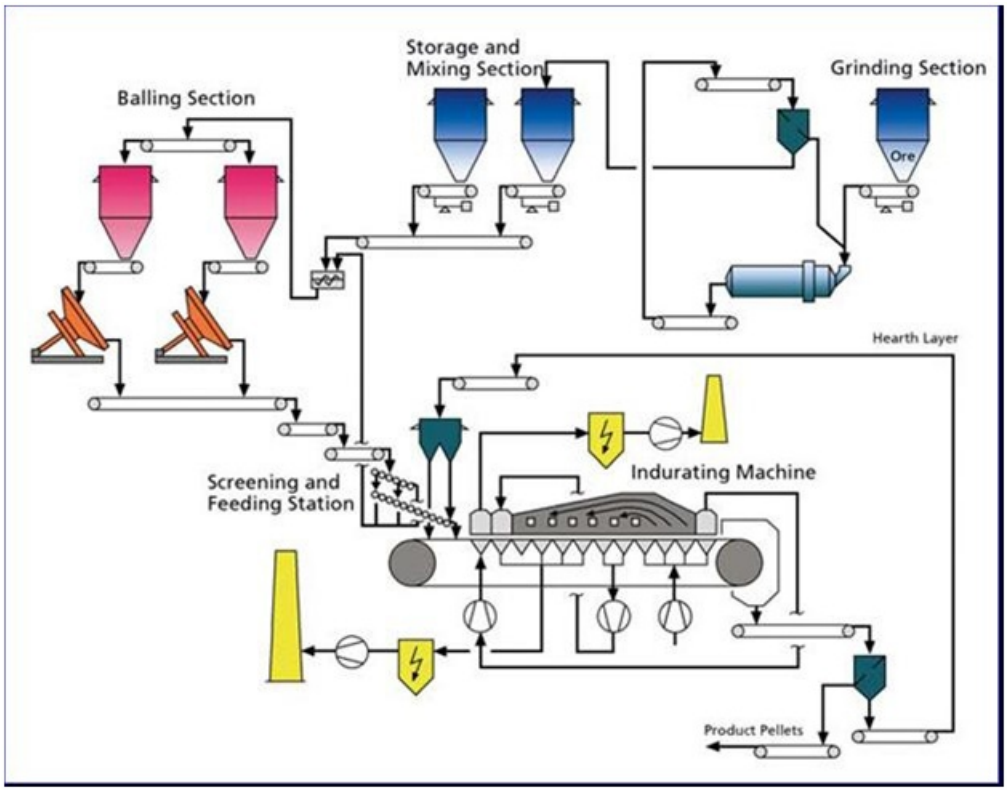

Figure 1.1: De-dusting system for sinter plant

In the selected dissertation the number of hood in ducting network is 39.The whole de-dusting system consists of three major parts as shown in fig. 1.2

Hood

Device used to ventilate the process equipment by capturing of air contaminants,which are then conveyed through exhaust system duct work to more convenient discharge point or to the air pollution control equipments.The quality of air required to capture and convey the air contaminants depends upon the size and shape of the hood, position relative to point of emission and the nature and quantity of air contaminants. The hood can generally classify into three main groups: enclosed, receiving and exterior hoods. Enclosures usually surrounded the point of emission, through sometimes one face may be partially or even completely open. Receiving hoods are those wherein the air contaminants are injected into hoods. Exterior hoods must capture air contaminants that are being generated from a point outside the hood itself, sometime some distance away. In this dissertation receiving type of rectangular hood is selected for receiving contaminated air from emission points.

Ducting network

The contaminated air from hood is carried from away from emission site to cyclonic separator or other filtering device by help of ducting circuits. The ducts arrangement

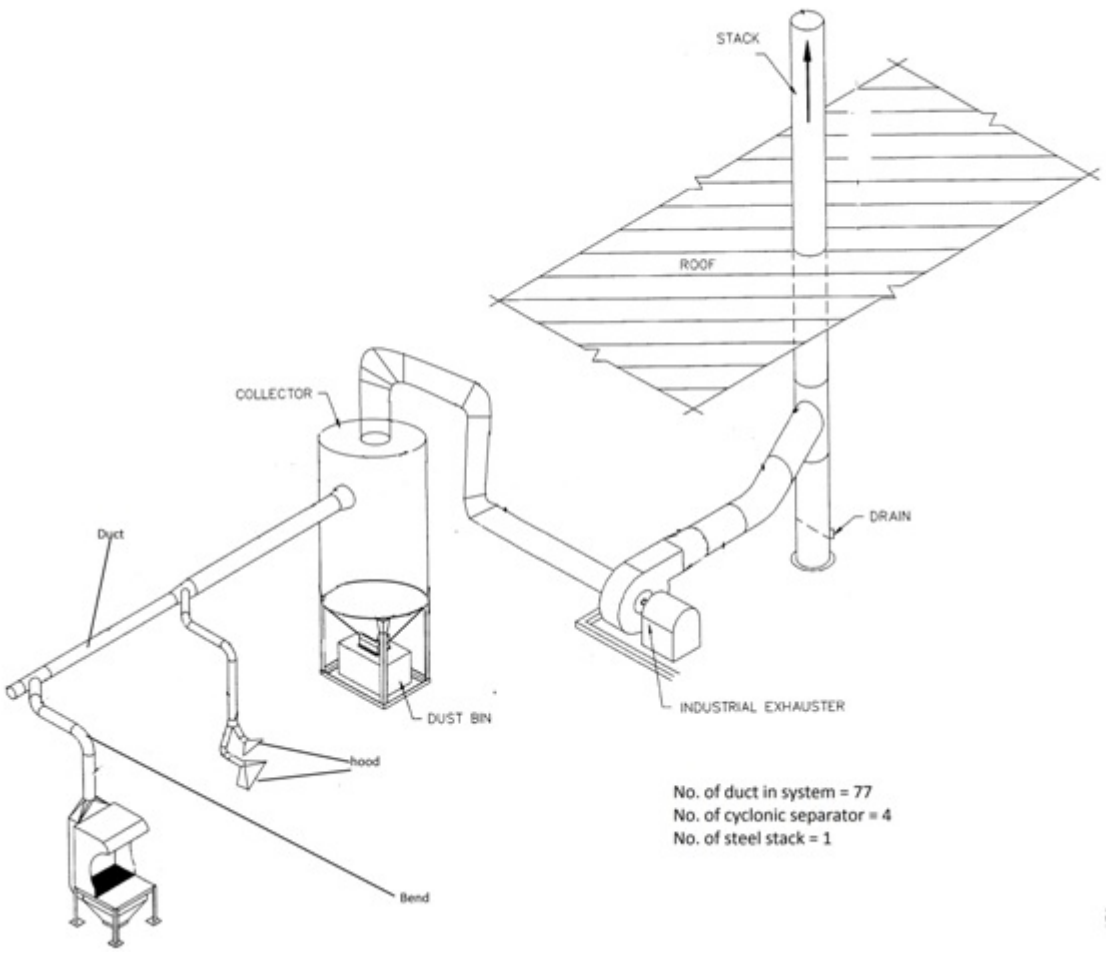

Figure 1.2: Major parts of de-dusting system

and routing is totally dependent on, site where de-dusting system is to installed, space available and also on pressure balancing.

Cyclonic separator

Device used to separate particulates material from fluid without use of filters. Rotational and gravitational effect used to separate solid and fluid. High speed rotating air flow is established within the cyclone. The air stream enters tangentially from the top of cyclone and moves towards bottom of cyclone in a helical pattern so, the heavy dust particle having more inertia strikes on the wall of cyclone and loses kinetic energy and stick to wall and as more and more dust particle accumulated, a layer is formed and it fall due to its own weight and get settle in the bottom of cyclonic separator and from bottom it is collected and removed.

Stack

The stack is a mechanical component that provides ventilation to the air which is free from contaminated dust particle. The height of stack is dependent on type of flue gas is going to exhausted in environment,and that is dependent on category of industry and Government norms and rules. The tall stack helps to self-neutralized the flue chemical components before it reaches the ground level.

1.2 Objective of dissertation

1. To design duct network subjected to external pressure as per ASME code and validate the result from PIPENET and PV Elite software.
2. To design cyclonic separator and validate the result from ANSYS CFX.
3. To design self supporting steel stack as per IS standard.

1.3 Methodology of dissertation

The design of duct network include the pressure drop balance inside each duct network, selection of safe thickness for duct, maximum span selection and stiffener design. The pressure drop balance in duct network is carried manually and result is verified from PIPENET software, selection of safe thickness and stiffener design is done through using ASME B31.3 and BPV code and verified by PV Elite software.Calculation of maximum safe span is done by using standard formula as mention in research paper.

The design of cyclonic separator is done by selecting different cyclone type, and selection of best model.Then mathematical modeling is done using two different model and finally selecting best model. 3D-modeling is done using INVENTOR using selected dimensions and the velocity at critical point is verified using ANSYS CFX. For design of fan pressure drop inside cyclonic separator is also find by using ANSYS CFX.

The design of self supporting steel stack is done by using IS:6533 (Part-1 and 2): 1989, IS 875 (Part-3 and 4): 1987, and IS 1893 (Part-4):2005, gives the basis for design and detailed procedure to determine static, dynamic and seismic loads coming on the structure.

1.4 Dissertation outline

Chapter 1: Includes introduction of de-dusting system for sinter plant.

Chapter 2: Includes literature review.

Chapter 3: Includes design of duct network.

Chapter 4: Includes design of cyclonic separator.

Chapter 5: Includes design of self supporting steel stack.

Chapter 6: Includes conclusion and future work.

Chapter 2

Literature review

The friction loss and dynamic loss associated with duct network is given in handbook of American Society of Heating, Refrigeration and Air conditioning Engineers (ASHRAE)[2] . The various parameters on which these losses depends are also described briefly.As friction loss which generally takes place along the length of pipes is given by Darcy and Colebrook but valid only for laminar flow. Later Stuart W. Churchill developed an equation by which friction factor for both laminar and turbulent flow can be easily found out. The dynamic loss is depending on number of factor like area of main and branch duct, flow through main and branch ducts, bends, fitting, damper etc. The procedure to find friction loss is given in ASHRAE handbook. From ASHRAE, standard types of bends, damper etc. are given according to requirement and of corresponding value of friction factor are found.

The design of duct thickness subjected to external pressure is described briefly in handbook of American Society of Mechanical Engineer (ASME B31.3)[3].For further design, given in code handbook to refer ASME BPV for pressure vessel subjected to external pressure.

The design of duct thickness subjected to external pressure is given in handbook of American Society of Mechanical Engineer (ASME BPV)[5].The duct network is subjected to atmospheric pressure and negative pressure inside the duct generated by fan so, design of duct is done considering these two pressure.Safe design, which depend upon various parameter like Youngs modolus of elasticity (E), Constant (A and B) calculated from the graph given in this code handbook, to find allowable pressure on the duct, to determine safety of duct.If the duct is fail due to external pressure the there are two option available, increase the thickness of duct or incorporate stiffener on ducts.

D.P Vakharia and Mohd. Frooq [6] worked on determination maximum span using maximum bending theory.The main objective of this paper to find numbers of supports required for15-km long pipeline.This paper consider weight of dust particle,weight of material of

pipe and weight of fluid flow as total weight or force coming on pipe for designing of supports and determining of number of supports required for 15 km pipline.

US Army Corps of Engineers[7] gave vast knowledge of to calculate maximum safe span of pipe which is used in liquid process piping.

ESSAR Piping stress analysis notes[8]Gave overview knowledge of stress generated in pipes.It also given the emperical formula for calculation of maximum safe span for duct system used in de-dusting system.By using the empirical formula given in this maximum safe span is calculated.

M.Heeumann, JR[13] described the dust collection devices .From the handbook description of cyclonic separator, bag filter and ESP etc are given.

EPC industrial manual[15] describes the working and principle associated with cyclonic separator.

Lingjuan Wang[16] worked on theoretical design of cyclonic separator. Design a cyclone separator system for particulate control, for it is necessary to accurately estimate cyclone performance. In this cyclone study, new theoretical methods for computing travel distance, numbers of turns and cyclone pressure drop have been developed. The flow pattern and cyclone dimensions determine the travel distance in a cyclone. The number of turns was calculated based on this travel distance. The new theoretical analysis of cyclone pressure drop was tested against measured data at different inlet velocities and gave excellent agreement. The results show that cyclone pressure drop varies with the inlet velocity, but not with cyclone diameter. Particle motion in the cyclone outer vortex was analyzed to establish a force balance differential equation. Barth's "static particle" theory, particle (with diameter of d50) collection probability is 50% when the forces acting on it, are balanced and combined with the force balance equation was applied in the theoretical analyses for the models of cyclone cut-point and collection probability distribution in the cyclone outer vortex. Cyclone cut-points for different dusts were traced from measured cyclone overall collection efficiencies and the theoretical model for calculating cyclone overall efficiency

The design of steel stack design subjected to wind load and other load is given in Bureau of Indian Standard, Indian Standard (IS:6533,Part-1and Part-2)[17][18]. As code covers the design of wind under static load and dynamic load.

The criteria for earth quake resistant design of structure is described in Bureau of Indian Standard, Indian Standard (IS:1893)[19]. As the earth quake effect is depends on terrain category on which the steel stack is going to install. In this code the description of all terrain category and design against seismic is described.

The design of steel stack against wind is explained in Bureau of Indian Standard, Indian Standard (IS:875)[20]. The basic analytical formula for wind load , basic mean wind

speed at different parts of Indian and various factor used for determining wind load can be obtained from this code.

Kirtikant Shaoo[21] explained analysis of self supporting steel chimney as per Indian standard.The objective of the study was to justify the code criteria with regard to basic dimensions of industrial steel chimney. A total of 66 numbers self supporting steel flared unlined chimneys with different top-to-base diameter ratio and height-to-base diameter ratio were considered for this study. The thickness of the chimney was kept constant for all the cases. Maximum bending moment and stress for all the chimneys were calculated for dynamic wind load as per the procedure given in IS 6533: 1989 (Part 2) using MathCAD software. Also the results were verified with the finite element analysis using commercial software ANSYS. Basic wind speed of 210 km/h which corresponds to coastal Orissa area is considered for these calculations. Maximum base moments and associated steel stresses were plotted as a function of top-to-base diameter ratio and height-to-base diameter ratio.

Chapter 3

Design of duct network

The dust laden air is enters from hood and travel through duct networks to cyclonic separator.There are losses associated with flow which are friction loss and dynamic loss. As the duct network goes on increasing means as the number of hood increases the possibility of flow of undesired amount of dust laden air increases through hood into duct network due to losses associated with flow. So there is a need of pressure drop balancing for duct networks.The pressure drop balancing is done according to ASHRAE handbook - system and equipments. As pressure drop is balanced inside each duct network then the desired flow is possible inside duct networks. The ducts is subjected to external pressure so, design of duct is done according to ASME B31.3 process piping and BPVC 1and 2. The objective of this part is to design the duct network for safe and proper functioning.The process flow diagram of duct network and predicted data as shown in fig. 3.1

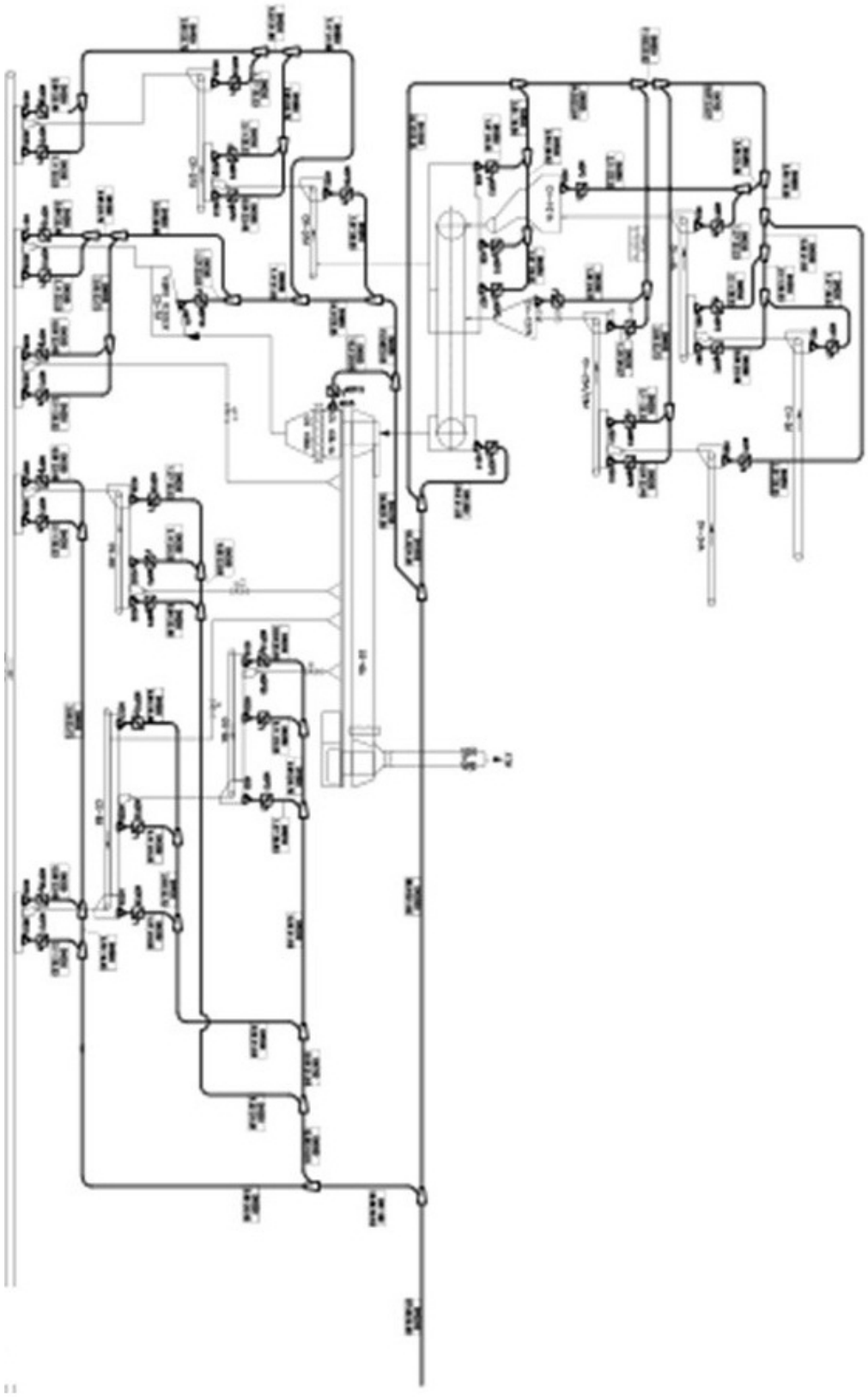

Figure 3.1: Process flow diagram

3.1 Overview

In duct network design the pressure drop balance is done by analytical method and result is verified by PIPENET software. As the duct is subjected to external pressure so, ASME code is used for designing for external pressure. Maximum safe span calculation and stiffener design as per ASME standard is covered in this portion.

3.2 Pressure drop balancing

Pressure balancing ensures the desired amount of flow inside the duct network. In case of small duct network there is no visible problem is identify related to desired amount of flow. But as the network increases, the flow from different hood is need not to give the desired amount of flow. To overcome this problem the pressure drop balancing inside ducting system is required. During balancing, if required altering in routing of duct network may be done and changes according to space constrain.

3.2.1 Duct system losses

Duct system losses are the irreversible transformation of mechanical energy into heat. The two types of losses :

1. Friction losses
2. Dynamic losses

3.2.1.1 Friction losses

Friction losses are due to fluid viscosity and as result of momentum exchange between molecules in laminar flow and between individual particles of adjacent fluid layers moving at different velocities in turbulent flow. Friction losses occur along the entire duct length. The pressure drop inside duct network is given by Darcy and S.W Churchill [2]as shown in eq. 3.1 :

$$\Delta \mathrm{P}_f = \frac{1000 f L V^2}{2D} \tag{3.1}$$

Where,

f =Darcy friction factor

L =Length (m)

V =Velocity of Fluid (m/s)

D =Diameter of duct (mm)

Within the region of laminar flow (Reynolds numbers less than 2000), the friction factor is a function of Reynolds number only. For completely turbulent flow, the friction factor depends on Reynolds number, duct surface roughness, joints. Between the bounding limits of hydraulically smooth behavior and fully rough behavior, is a transitional roughness zone where the friction factor depends on both roughness and Reynolds number. In this transitionally rough, turbulent zone the friction factor f is calculated by Colebrook's equation (Colebrook 1938-39)[2] as given in eq.3.2

$$\frac{1}{\sqrt{f}} = -2log(\frac{12\varepsilon}{3.7D_h} + \frac{2.51}{R_e\sqrt{f}}) \tag{3.2}$$

Where,

ε=Roughness factor (mm)

R_e =Reynolds number

D_h =Hydrodynamic diameter (mm)

As the Colebrook's equation cannot be solved explicitly for f , S.W Churchill developed a equation for calculation of friction factor.[2]

$$f = 8[(\frac{8}{R_e})^{12} + (A+B)^{-1.5}]^{\frac{1}{12}} \tag{3.3}$$

$$A = [-2.457ln\{(\frac{7}{R_e})^{0.9} + 0.27\frac{\varepsilon}{D}\}]^{16} \tag{3.4}$$

$$B = (\frac{37530}{R_e})^{16} \tag{3.5}$$

Where,

A and B = Churchill constant

3.2.1.2 Dynamic losses

Dynamic losses result from flow disturbances caused by duct mounted equipment and fittings that change the airflow path's direction and/or area. These fittings include entries, exits, elbows, transitions, and junctions. Idelchik et al. (1986) [2]discuss parameters affecting fluid resistance of fittings and presents local loss coefficients. The dimensionless coefficient C is used for fluid resistance, because this coefficient has the same value

in dynamically similar streams (i.e., streams with geometrically similar stretches, equal Reynolds numbers, and equal values of other criteria necessary for dynamic similarity). The fluid resistance coefficient represents the ratio of total pressure loss to velocity pressure at the referenced cross section .

$$C = \frac{\Delta \mathrm{P}_j}{P_v} \tag{3.6}$$

Dynamic losses occur along a duct length and cannot be separated from friction losses. For ease of calculation, dynamic losses are assumed to be concentrated at a section (local) and to exclude friction. Frictional losses must be considered only for relatively long fittings. Generally, fitting friction losses are accounted for by measuring duct lengths from the center line of one fitting to that of the next fitting. For fittings closely coupled (less than six hydraulic diameters apart), the flow pattern entering subsequent fittings differs from the flow pattern used to determine loss coefficients. Adequate data for these situations are unavailable. For all fittings, except junctions, calculate the total pressure loss $\Delta \mathrm{P_j}$ at a section is calculated by eq. 3.7:

$$\Delta \mathrm{P}_j = C_o.P_{v,o} \tag{3.7}$$

where the subscript o is the cross section at which the velocity pressure is referenced. The dynamic loss is based on the actual velocity in the duct, not the velocity in an equivalent non-circular duct. For unequal area fittings, convert a loss coefficient from section o to section i using eq. 3.8.

$$C_i = \frac{C_o}{(\frac{V_i}{V_o})^2} \tag{3.8}$$

For converging and diverging flow junctions, total pressure losses through the straight (main) section are calculated by eq.3.9

$$\Delta \mathrm{P}_j = C_{c,s}.P_{v,c} \tag{3.9}$$

For total pressure losses through the branch section :

$$\Delta \mathrm{P}_j = C_{c,b}.P_{v,c} \tag{3.10}$$

where $\mathrm{p_{v,c}}$is the velocity pressure at the common section c, and $\mathrm{C_{c,s}}$ and $\mathrm{C_{c,b}}$ are losses for the straight (main) and branch flow paths, respectively, each referenced to the velocity pressure at section c. To convert junction local loss coefficients referenced to straight and branch velocity pressures, use the eq.3.11

$$C_i = \frac{C_{c,i}}{(\frac{V_i}{V_c})^2} \tag{3.11}$$

The junction of two parallel streams moving at different velocities is characterized by turbulent mixing of the streams, accompanied by pressure losses. In the course of this mixing, an exchange of momentum takes place between the particles moving at different velocities, resulting in the equalization of the velocity distributions in the common stream. The jet with higher velocity loses a part of its kinetic energy by transmitting it to the slower moving jet. The loss in total pressure before and after mixing is always large and positive for the higher velocity jet and increases with an increase in the amount of energy transmitted to the lower velocity jet. Consequently, the local loss coefficient, will always be positive. The energy stored in the lower velocity jet increases as a result of mixing. The loss in total pressure and the local loss coefficient can, therefore, also have negative values for the lower velocity jet (Idelchik et al. 1986).[2]

3.3 Safe thickness selection

As the duct is subjected to external pressure , there is need to design the duct which can sustain that much of external pressure. The design of duct is carried out according to ASME B31.3 process piping for external pressure, which states to refer ASME BPVC Section VIII division I code for design of pressure vessel for external pressure.As the duct which subjected to negative pressure from inside, and atmospheric pressure from outside, the system will acts as external pressurized pressure vessel. As the component is subject to external pressure it is mandatory to take special care of it during designing, if not there is chance of buckling of duct may be seen which results in collapse of ducting network. So thickness calculation of ducts subjected to external pressure is done according to ASME code B31.3 process piping. To determine the wall thickness for straight pipe under external pressure is explain in Para 304.1.3 and procedure described in BPVC code section VIII division I, UG 28 .

Assume the thickness (t) of the duct and determine the ratio of D_o/t and L/D_o.

To find value of "A". (ref. FIG. G of ASME section VIII, part D).

To find the value of "B". (ref. FIG. CS-1 of ASME section VIII, part D).

To find the maximum external allowable working pressure , which is given in eq. 3.12

$$P_a = \frac{4B}{3(\frac{D_o}{t})} \tag{3.12}$$

Or if the value of "A" falls on left of the applicable material/temperature line, the value of can be calculated using eq. 3.13

$$P_a = \frac{2AE}{3(\frac{D_o}{t})} \tag{3.13}$$

If the value of allowable pressure (P_a) > external pressure (P) then selected thickness of pipe is safe otherwise increase thickness.

3.4 Maximum safe span selection

After calculating the safe thickness, it required to calculate the maximum safe span .The safe span depends on various parameters like deflection permitted, modulus of elasticity, moment of inertia and total weight. The total weight includes all weight i.e. Weight of pipe, weight of fluid and weight of dust accumulated. In general considering 30% to 40% of dust gets accumulated in pipes. The formula of maximum safe span is given in eq. 3.14

$$L = [\frac{yEI}{17.1W}]^{\frac{1}{4}} \tag{3.14}$$

Where,

I =Moment of inertia = $\frac{\pi}{64}(D_o^4 - D_i^4)$

W =Total weight = $W_f + W_d + W_m$

W_f =Weight of fluid

W_d =Weight of dust particle = $\frac{\pi}{4}(D_i^2).\rho_d.(0.3)$

W_m =Weight of material

y =Permitted deflection (mm)

If the value of L_{max} > L then, supports can apply on extreme point.

If the value of L_{max} < L then, number of supports with in the length must increase.

3.5 Stiffener design

As the external pressure exceed the allowable pressure then the external pressure caused the duct to buckled. So, need to increased the thickness. There is another way to make the duct safe by applying stiffning ring around the duct which is going to fail . The procedure of stiffening ring design is explain in ASME BPV code.

$$I_s = [D_o^2 L_s(t + \frac{A_s}{L_s})A]/14 \tag{3.15}$$

$$B = \frac{3}{4}\left(\frac{P.D_o}{t + \frac{A_s}{L_s}}\right) \tag{3.16}$$

$$A = \frac{2B}{E} \tag{3.17}$$

If I $>$ I_sThen stiffener design sustain external pressure.

If I $<$ I_sThe stiffener design cannot sustain external pressure.

Where,

I =Moment of inertia of stiffener

Table 3.1: Stiffener design for ducts

Branch	D_o	t	A_s	L_s	A_s/L_s	I	B	A	I_s	Comment
14-p	1219.2	8	3300	5000	0.66	6187500	11.16074827	0.000114399	525934.0511	Safe
l-p	1016	8	3300	16500	0.2	6187500	9.822365854	0.00010068	1004387.945	Safe
p-q	1616	8	3300	2500	1.32	6187500	13.74553648	0.000140893	612351.0986	Safe
q-20	2016	8	3300	12500	0.264	6187500	19.33910939	0.000198228	5944536.797	Safe

3.6 Data for calculation

1. The calculation of friction loss and dynamic loss is calculated by considering roughness factor 0.05 mm , material selected is SA 516 Gr 70 and density of fluid is 1.2 kg/m^3. The calculation of different duct is given in Appendix (A1.1 and A1.2) .

2. The calculation of thickness is done by considering material SA 516 Gr 70 and modulus of elasticity at given temperature is 195120 MPa. The calculation is given in Appendix (A1.3) .

3. The calculation of maximum safe span is given in Appendix (A1.4) .The following data is consider for calculation Density of Material - 7850 Kg/m^3, Density of Dust Particle -1000 Kg/m^3, Density of Fluid -1.2041 Kg/m^3 , Deflection - 12.5 mm , Modulus of Elasticity - 195120 MPa, Temperature - 100^{0}C .

3.7 Verification from software

3.7.1 Pressure drop verification from PIPENET software

The pressure drop in each duct circuit is work out analytically and the result is verified by using PIPENET software. The graph shows pressure drop in each duct as shown in fig. 3.2

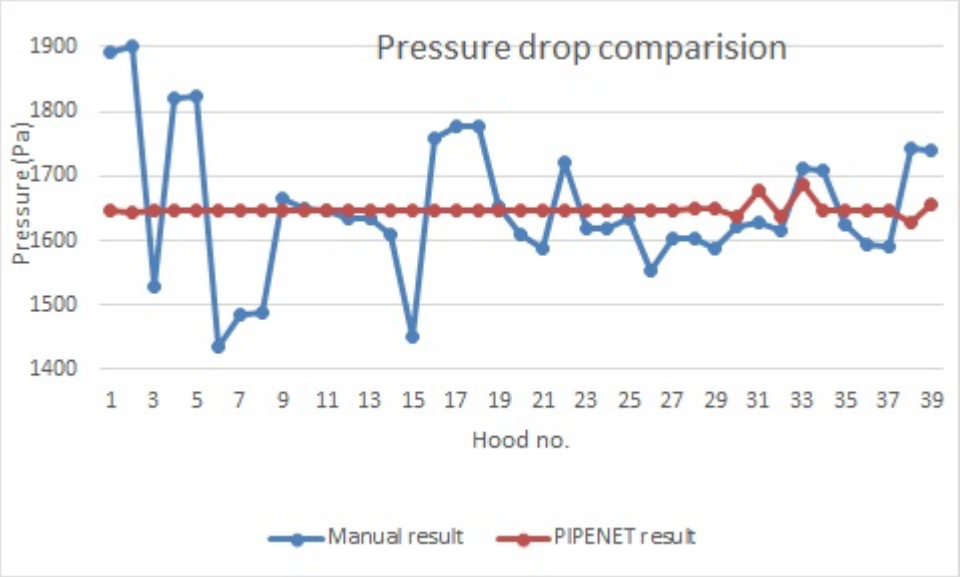

Figure 3.2: Pressure drop in various ducts

From the above graph it is found that the variation in pressure drop in analytical and PIPENET software below 15%. So desired amount of flow will be possible.

3.7.2 Flow rate comparison

The mass flow rate as predicted manually is compare with flow obtained from PIPENET result. It is found that the different in result of mass flow rate calculated manually and by using PIPENET software is hardly havig difference of 5% . As predicted and actual mass flow rate is coming same as result of pressure drop balance so, the hole duct network is said to be balance. The graph of comparison is shown in fig. 3.3

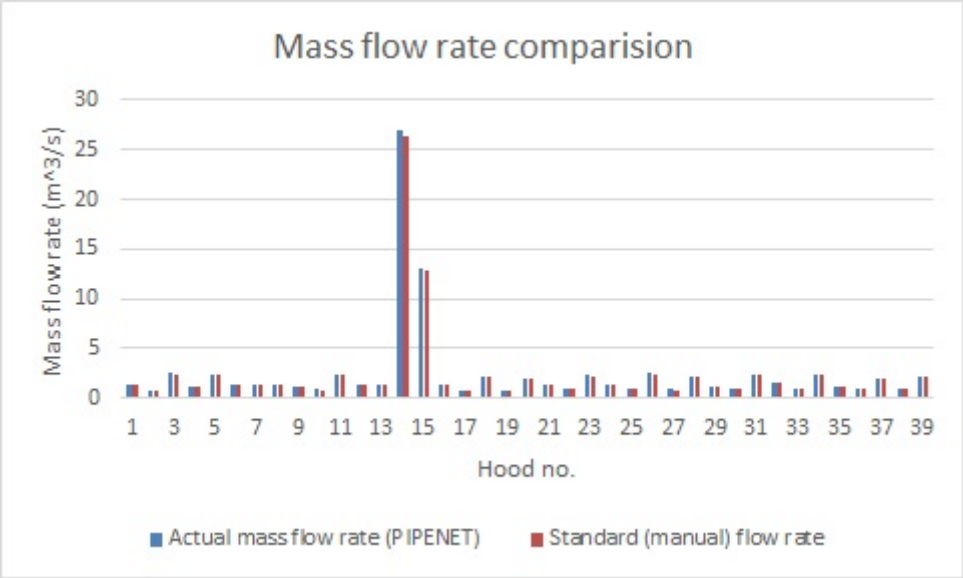

Figure 3.3: Mass flow rate comparison

Chapter 4

Design of cyclonic separator

The dust laden gases cannot release directly into the atmosphere. So there is a need of design of such a device which removes dust particle form dust laden air. Therefore design of cyclonic separator is one of the best methods for dust collection at low cost. There are different model suggested for cyclonic separator design for industry (Lapple and Licht)[14]. The objective of this part is to design cyclonic separator by different model and select the best one suite the requirement.

4.1 Overview

Cyclone separators provide a method of removing particulate matter from air streams at low cost and low maintenance. In general, a cyclone consists of an upper cylindrical part referred to as the barrel and a lower conical part referred to as cone . The air stream enters tangentially at the top of the barrel and travels downward into the cone forming an outer vortex as shown if fig. 4.1. The increasing air velocity in the outer vortex results in a centrifugal force on the particles separating them from the air stream. When the air reaches the bottom of the cone, an inner vortex is created reversing direction and exiting out the top as clean air while the particulates fall into the dust collection chamber attached to the bottom of the cyclone.

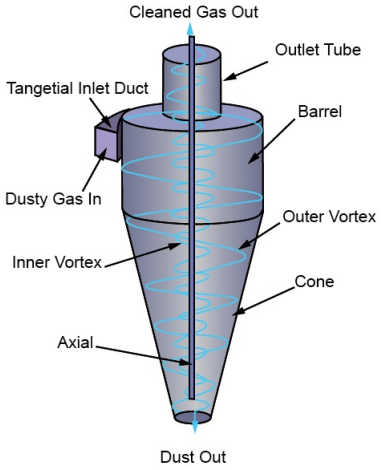

Figure 4.1: Cyclonic separator

4.2 Basic standard design of industrial cyclone

Standard configuration of industrial cyclones for particulates removal are available resulting from compilation of many empirical measurements. Cyclones for other applications (for eg. industrial hygiene or pharmaceutical) are usually custom designs. Generally are grouped into three classes: high efficiency, medium efficiency and general purpose. All dimensions listed are normalized to the cyclone's body diameter. Fig. 4.2 shows basic notations of cyclonic separator. The various standard ratio is given in table 4.1from that basic dimensions of cyclonic separator are find out.

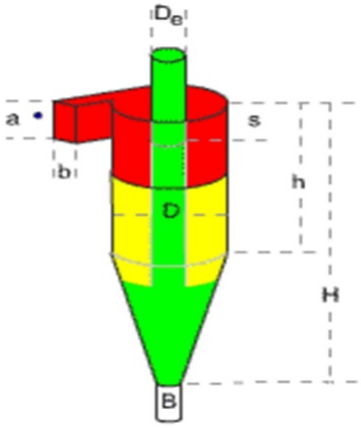

Figure 4.2: Basic notations of cyclone

Table 4.1: Standard design of industrial cyclone

			High efficiency		Medium efficiency		General purpose
Symbol	Description		Stairmand	Swift	Shephard and Lapple	Swift	Peterson and Whitby
D	Body diameter		2.8	2.8	2.8	2.8	2.8
a	Inlet height	K_a=a/D	0.55	0.44	0.5	0.5	0.583
b	Inlet width	K_a=a/D	0.2	0.21	0.25	0.25	0.208
s	Outlet length	K_a=a/D	0.5	0.5	0.625	0.6	0.583
D_e	Gas outlet diameter	K_a=a/D	0.5	0.4	0.5	0.5	0.5
h	Cylinder height	K_a=a/D	1.5	1.4	2	1.75	1.33
H	Overall height	K_a=a/D	4	3.9	4	3.75	3.17
B	Dust outlet diameter	K_a=a/D	0.375	0.4	0.25	0.4	0.5
K	Configuration No.		551.3	699.2	402.9	381.8	342.3
N_{sh}	Inlet velocity head		6.4	9.24	8	8	7.76
Surf	Surface parameter		3.67	3.57	3.78	3.65	3.2
N_H surf			23.5	21.2	13.3	13.1	13.8

4.3 Different model of cyclonic separator

4.3.1 Lapple model (Classical cyclonic design)

Th Lapple model of cyclonic design process, was developed by Lapple in the early 1950s. The Lapple model process is perceived as a standard method and has been considered by some engineers to be acceptable. However, there are several problems associated with this design procedure. Lapple model designing process does not consider the cyclone inlet velocity in developing cyclone dimensions. It was reported (Parnell, 1996) [16]that there is an "ideal" inlet velocity for the different cyclone designs for optimum cyclone performance. Lapple model does not predict the correct number of turns for different type of cyclones. The overall efficiency predicted by the Lapple model process is incorrect because of the inaccurate fractional efficiency curve generated by the Lapple model process . In order to use the Lapple model design process, following knowledge must required :

1. Flow conditions
2. Particulate matter (PM) concentrations and particle size distribution (PSD)
3. The type of cyclone to be designed (high efficiency, conventional, or high)

The cyclone type will provide all principle dimensions as a function of the cyclone barrel diameter (D). With these given data, the Lapple model design process is as follows

4.3.1.1 Number of effective turns

Lapple modal design process starts with calculation of number of effective turns. The number of effective turns in a cyclone is the number of revolutions the gas spins while

passing through the cyclone outer vortex. A higher number of turns of the air stream result in a higher collection efficiency. The Lapple model for n_t calculated by eq. 4.1

$$n_t = \frac{1}{a}[h + \frac{(H-h)}{2}] \tag{4.1}$$

Where,

a =Inlet height (m)

h =Cylinder portion height (m)

H =Total height of cyclone (m)

4.3.1.2 Cut diameter

The second step of the Lapple model process is the calculation of the cut-point diameter. The cut-point of a cyclone is the aerodynamic equivalent diameter (AED) of the particle collected with 50% efficiency. As the cut-point diameter increases, the collection efficiency decreases .The Lapple cut-point model was developed based upon force balance theory. The Lapple model for cut-point ($[d_p]_{cut}$) is calculated by eq. 4.2

$$[d_p]_{cut} = \sqrt{\frac{9\mu_g b}{2\pi n_t V_i(\rho_p - \rho_g)}} \tag{4.2}$$

In the process to develop this cut-point model, it was assumed that the particle terminal velocity was achieved when the opposing drag force equaled the centrifugal force, and the drag force on every single particle was determined by Stokes law. As a result, the cut-point ($[d_p]_{cut}$) determined by the Lapple model (equation 4.2) is an equivalent spherical diameter (ESD), or in other words, Stokes diameter. The following equation can be used to convert ESD to AED for the spherical particles:

$$AED = \sqrt{\rho_p}.ESD \tag{4.3}$$

Since $\rho_p >> \rho_g$, it could be considered that (ρ_p-ρ_g) $\approx \rho_p$. Combining equations 2 and 3, the Lapple model for cut-point could be modified as follows:

$$[d_p]_{cut} = \sqrt{\frac{9\mu_g b}{2\pi n_t V_i \rho_p}} \tag{4.4}$$

where,

μ_g =Viscosity of gas (kg/m-s)

b = Width of inlet (m)

n_t =No. of effective turn

V_i =Inlet velocity (m/s)

ρ_p =Density of dust particle (kg/m^3)

V_i =Inlet velocity (m/s)

ρ_p =Density of dust particle (kg/m^3)

ρ_g =Density of gas (kg/m^3)

Equation 4.4 is the Lapple model for cut-point in AED. This model indicates that the cut-point is totally independent of characteristics of the inlet PM. However, It has been reported that the cyclone fractional efficiency curves are significantly affected by the particle size distribution of particulate matter entering.

4.3.1.3 Collection efficiency

The third step of Lapple model process is to determine the collection efficiency. Based upon the cut-point, Lapple then developed an empirical model (eq.4.5) for the prediction of the collection efficiency for any particle size, which is also known as fractional efficiency curve:

$$\eta_c = \frac{1}{1 + (\frac{[d_p]_{cut}}{d_{pj}})} \tag{4.5}$$

4.3.1.4 Overall efficiency

If a size distribution of the inlet particles is known, the overall collection efficiency of a cyclone can be calculated based on the cyclone fractional efficiency. The overall collection efficiency of a cyclone is the weighted average of the collection efficiencies for the various size ranges. It is given by:

$$\eta_o = \eta_c.m_c \tag{4.6}$$

4.3.1.5 Pressure drop

Cyclone pressure drop is another major parameter to be considered in the process of designing a cyclone system. Pressure drop is calculated analytically or it can be find out by CFD analysis.

4.3.1.6 Design as per Lapple model

The basic dimensions of cyclonic separator for different cyclonic type is calculated from the table 4.1 is given in table 4.2:

Table 4.2: Basic dimension of different cyclonic type

Cyclonic type	a (m)	b (m)	s (m)	D_e (m)	h (m)	H (m)	B (m)
Stairmand	1.4	0.56	1.4	1.4	4.2	11.2	1.05
Swift high	1.232	0.588	1.4	1.12	3.92	10.92	1.12
Shephard and Lapple	1.4	0.7	1.75	1.4	5.6	11.2	0.7
Swift general	1.4	0.7	1.68	1.4	4.9	10.5	1.12
Peterson and whitby	1.6324	0.5824	1.6324	1.4	3.724	8.876	1.4

Now using equation 4.1, 4.4 and 4.5 different parameter of cyclonic model according to Lapple model is designed. The parameter calculated given in table4.3

Table 4.3: Lapple's model parameter

Cyclone type	n_t	V_i(m)	$[d_p]_{cut}$ (μm)	Collection efficiency (%)				
				0.2 μm	0.5 μm	1 μm	3 μm	100 μm
Stairmand	5.5	31.18	21.6	0.9	2.2	4.4	12.1	82.23
Swift high	6.02	33.75	8.6	2.2	5.4	10.4	25.8	92.08
Shephard and Lapple	6.0	24.94	11.04	1.7	4.3	8.3	21.3	90.05
Swift general	5.5	24.94	11.6	1.6	4.1	7.9	20.5	89.6
Peterson and Whitby	3.85	25.71	12.38	1.58	3.8	7.4	19.5	88.98

4.3.2 Licht model

The Lapple model is not consider turbulent flow. So a new theory base on turbulent flow is developed by Licht with lateral mixing.

4.3.2.1 Pre-factor

The pre- factor in Licht model is determined by eq. 4.7

$$A = 2[\frac{KQ\rho_p(n+1)}{18\mu_g D^3}]^{\frac{1}{2(n+1)}} \tag{4.7}$$

Where,

K =Configuration factor

Q =Volume flow rate (m^3/s)

ρ_p =Density of dust particle (kg/m^3)

n =Vortex exponent

μ_g =Density of gas (kg/m^3)

D =Diameter of cyclone (m)

4.3.2.2 Cut diameter

In Licht model cut diameter for 50% collection efficiency is determined by eq. 4.8

$$d_{p50\%} = (\frac{0.693}{A})^{n+1} \tag{4.8}$$

Where,

A =Pre-factor

4.3.2.3 Collection efficiency

Licht had developed a empirical formula for finding collection efficiency which is depends on cut diameter for 50% collection efficiency and vortex exponent.It is given by eq. 4.9

$$\eta = 1 - exp[-0.693(\frac{d_{pj}}{d_{p50\%}})^{\frac{1}{n+1}}] \tag{4.9}$$

Where,

d_{pj} =Diameter of particle (µm)

$d_{p50\%}$ =Cut dia. for 50% collection efficiency (µm)

4.3.2.4 Overall efficiency

The overall efficiency of Licht model is calculated by eq. 4.10

$$\eta_o = \eta_i.f_j \tag{4.10}$$

Where,

η_i=Collection efficiency

f_j =Fraction of size range

4.3.2.5 Design as per Licht model

The different parameter is calculated by using equation 4.7, 4.8 and 4.9 . The parameter for different cyclonic type is given in table 4.4

Table 4.4: Licht model parameter

Cyclonic type	A	$d_{p50\%}$ (µm)	Collection efficiency (%)				
			0.2 (µm)	0.5 (µm)	1 (µm)	3 (µm)	100 (µm)
Stairmand	973.48	2.65	14.80	23.68	32.95	52.44	99.53
Swift high	1041.02	2.3	16.01	25.38	35.14	55.29	99.70
Shephard and Lapple	891.02	3.10	13.70	21.91	30.64	49.35	99.27
Swift general	877.59	3.18	13.50	21.84	30.27	48.85	99.20
Peterson and Whitby	850.95	3.36	13.14	21.05	29.50	47.79	99.09

As height for cyclonic separator is design constraint. Means the height must keep small for better stability and economical point of view, so Peterson and Whitby [14]cyclonic type is selected over others cyclonic type. And from given two mathematical model Licht model is selected over Lapple because of following reason:

1. This model does n't consider turbulent flow. As the flow at entry of cyclone is turbulent in nature.

2. The collection efficiency of Lapple model for very small dust particle is very low as compare to Licht model.

4.3.3 Software verification

3D modeling

The 3D modeling of Licht model is prepared by using Inventor as shown in fig.4.3 and basic dimension selected is of Peterson and Whitby cyclonic type as shown in table 4.5

Table 4.5: Basic dimension as per Peterson and Whitby

Cyclonic type	a (m)	b (m)	s (m)	D_e (m)	h (m)	H (m)	B (m)
Peterson and whitby	1.6324	0.5824	1.6324	1.4	3.724	8.876	1.4

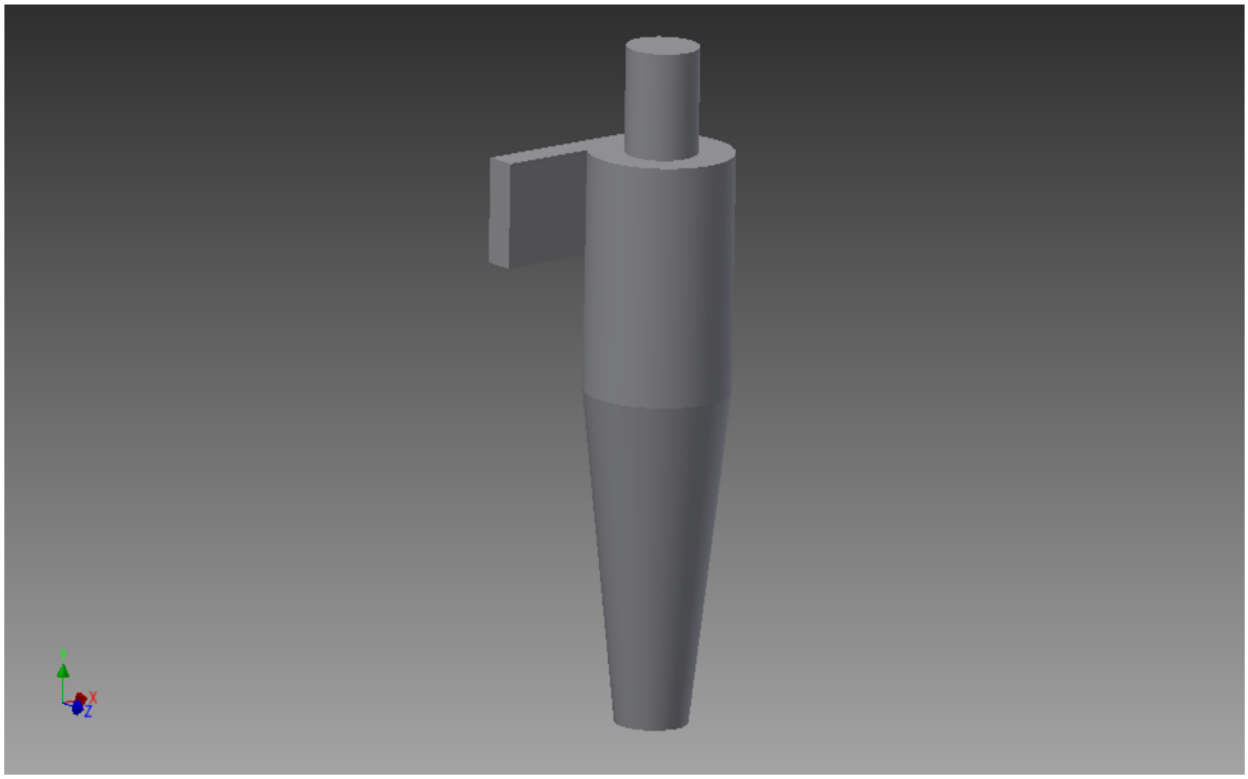

Figure 4.3: 3D model of cyclonic separator

Velocity verification by ANSYS CFX

The velocity of dust laden air at inlet must be in between 20 to 25 m/s and at exit, it must be in between 15 to 20 m/s as per standard otherwise if the velocity is greater than the given velocity range the erosion of cyclonic material takes place and also there is a chance of increase of vibration in cyclonic separator. In CFX, IGES file is imported for further analysis. The meshing is created with tetrahedral element as shown in 4.4. The boundary condition (i.e flow at inlet and pressure at outlet) is applied and the velocity range is determined using CFX analysis.

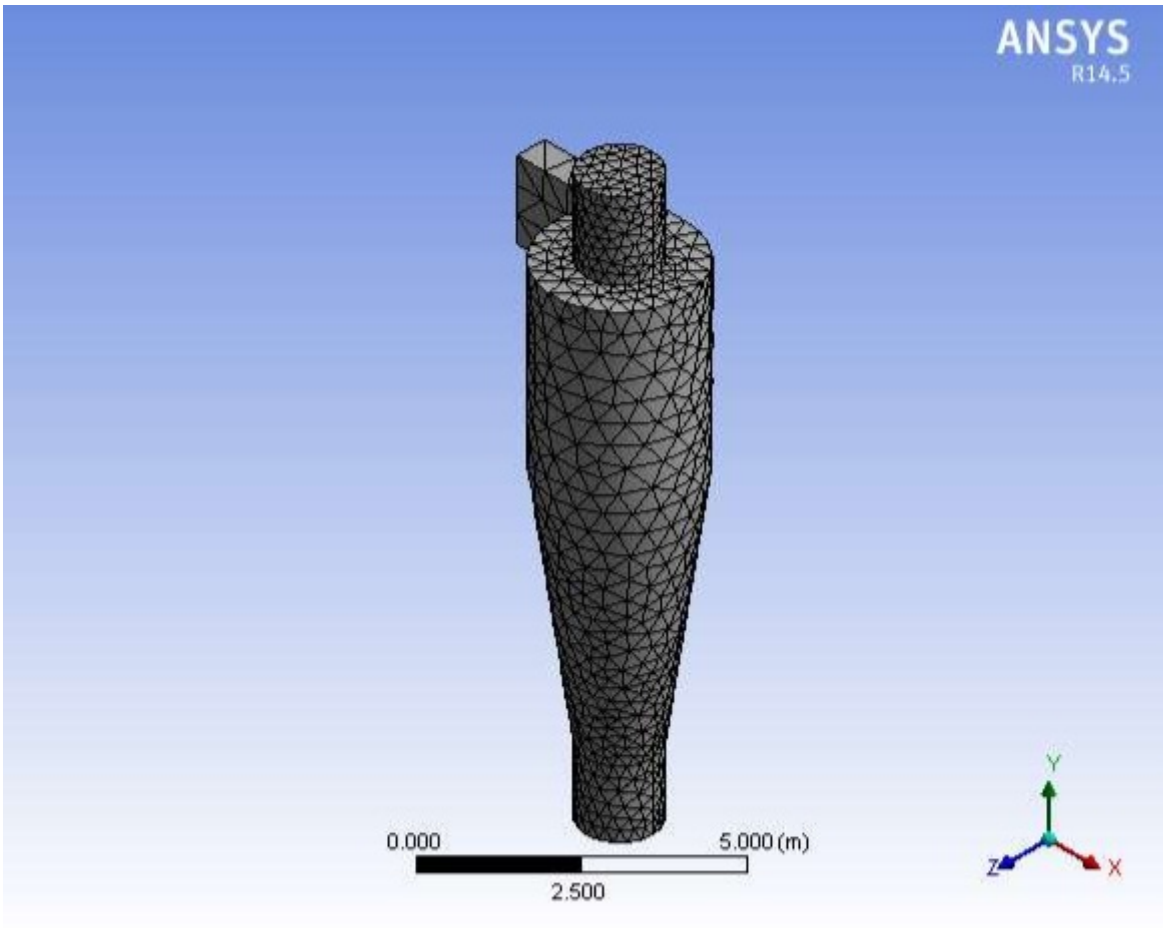

Figure 4.4: Mesh generation

The velocity profile after CFX analysis as shown in fig. 4.5. The velocity at critical points are given in table 4.6

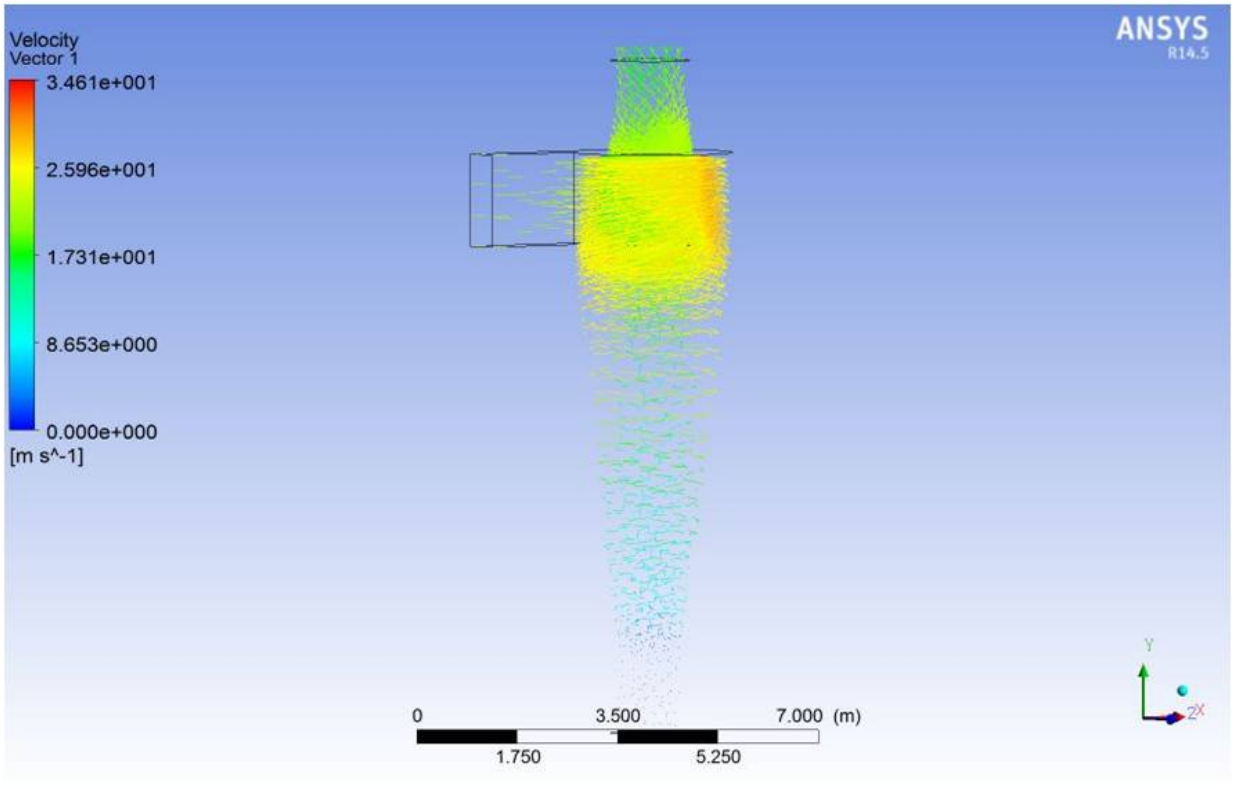

Figure 4.5: Velocity analysis

Table 4.6: Velocity at critical points

Position	Inlet	Outlet	At first strike	Cone
Velocity (m/s)	24.4	17.3	33	8.6

Pressure drop calculation from ANSYS CFX

The pressure drop is the difference between the pressure at inlet and outlet of cyclonic separator is determined for selection of fan. In CFX by applying boundary condition (i.e flow at inlet and pressure at outlet) the pressure drop is determined. From fig.4.5 the pressure difference is found to be 985 Pa as shown in fig. 4.6

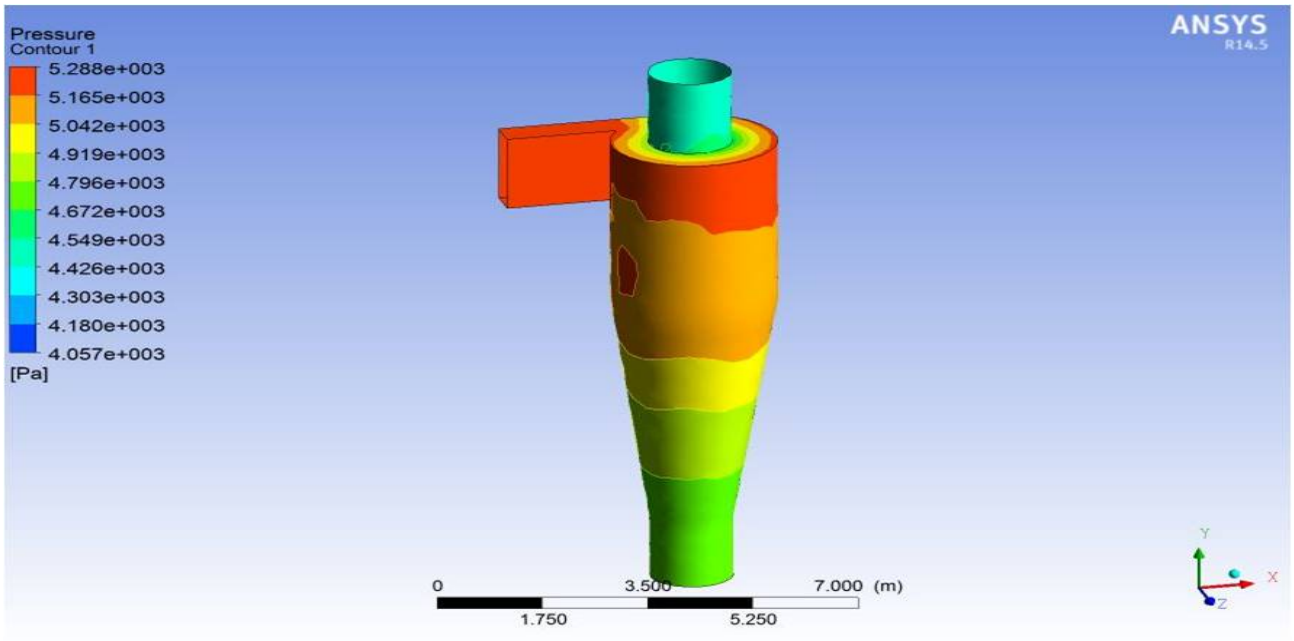

Figure 4.6: Pressure drop analysis

Chapter 5

Design of self supporting steel stack

The dust laden gases forced by fan into stack for safely emission of clean gases into atmosphere from a certain height .So there is a need for design of stack. Most of the industrial steel stack are tall structures having circular cross-sections. Such a slender, lightly damped structures are prone to wind-exited vibration. Also Geometry of a self supporting steel stack plays a vital role in its structural behavior under lateral dynamic loading. This is because geometry is primarily responsible for the stiffness parameters of the stack or simply say stiffness of the stack. However, basic dimensions of industrial self supporting steel stack, such as height, diameter at exit, etc., are generally derived from the associated environmental conditions . To ensure a desired failure mode design code (IS-6533, 1989 Part 2) imposes several criteria on the geometry (top-to-base diameter ratio and height-to-base diameter ratio) of steel chimneys. The objective is to study the code and design a steel stack for safe emission on gases for sinter plant.

5.1 Overview

Self supporting steel stack subjected to various loads in vertical and lateral direction. Important loads that a steel stack often experiences are wind loads, earthquake loads, and temperature loads apart from self weight, loads from the attachments, imposed loads on the service platforms. Wind effects on stack plays an vital role on its safety as steel stack are generally very tall structures. The circular cross section of the stack experiences aerodynamic lift by wind load.Also seismic load is a major consideration for stack as it is considered as a natural load. Seismic load is generally dynamic in nature. According to code provision quasi-static methods are used for evaluation of this load and recommend amplification of the normalized response of the stack with a factor that depending on the soil and intensity of earthquake. In general flue gases with very high temperature released inside a chimney. Due to this high temperature a temperature gradient with respect to ambient temperature outside is developed and hence stresses in the stack may

be generated. Therefore, temperature effects on stack is also important factor to be considered in the design of steel stack. This chapter describes the wind load and seismic load effects on self-supporting steel stack.In general self supporting steel stack have two major portion flare and cylindrical portion.The flare is conical in shape provided for better stability of steel stack.The self supporting steel stack is shown in fig. 5.1

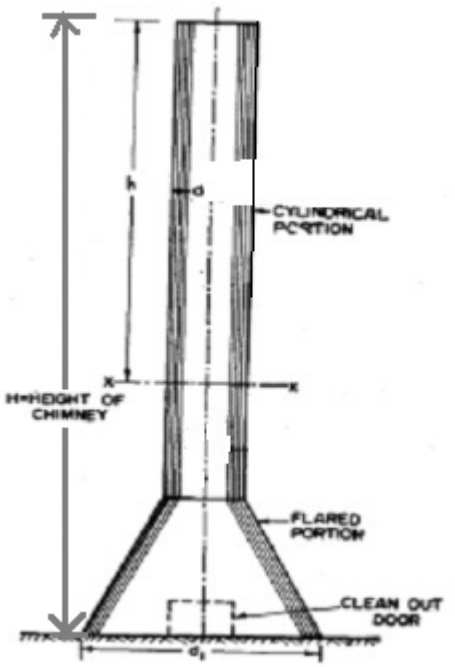

Figure 5.1: General steel stack

5.2 Wind engineering

For self-supporting steel stack, wind is considered as major source of loads. This load can be classified into two components respectively :

1. Along-wind effect
2. Across wind effect

The wind load exerted at any point on a steel stack is considered as the sum of quasi-static and a dynamic-load component. The static-load component is that force which, wind will exert if it blows at a mean (time-average) steady speed and which will tend to produce

a steady displacement in the structure (stack). The dynamic component, which causes oscillations of a stack, and it is generated due to the following reasons:

1. Gusts
2. Vortex shedding
3. Buffeting

5.2.1 Along wind effects

Along wind effects are produce by the drag component of the wind force on the stack.When wind flows on the face of the structure/stack, a direct buffeting action are produced. To estimate such type of loads it is required to model the chimney as a cantilever and fixed to the ground. In the model the wind load is acting on the face of the stack , which is expose to wind, so create predominant moments. But a problem is that wind does not blow at a fixed rate every time. So the corresponding loads results in dynamic nature. For evaluation , along wind loads the stack is modeled as bluff body with turbulent wind flow. In Indian standard code IS: 6533,1989, equivalent static method is used for estimating these loads. In this procedure the wind pressure is determined which acts on the face of the stack as a static wind load. Then it is amplified using gust factor for calculation of the dynamic effects.

5.2.2 Across wind effects

Across wind effect is not fully solved and it is required a further research work on it. For design of self supporting steel stack, Indian standard remain silent about it. But it is mentioned in IS 4998 (part 1), 1992 and ACI 307-95 which is applicable for concrete chimney only. Also CICIND code does not mention this effects and depends on IS 4998 (part 1), 1992 and ACI 307-95. Generally stack-like tall structures are considered as bluff body and oppose to a streamlines. When the streamlined body causes the oncoming wind flow, the bluff body causes the wind to separate from the body. Due to this a negative regions are formed in the wake region behind the stack. This wake region produces highly turbulent region and forms high speed eddies called vortices. These vortices alternatively forms lift forces and it acts in a direction perpendicular to the incident wind direction. Stack oscillates in a direction perpendicular to the wind flow due to this lift forces.

5.3 Wind load calculation

According to IS 875 (part 3),1987 basic wind speed can be calculated by eq. 5.1

$$V_z = K_1 K_2 K_3 V_b \tag{5.1}$$

Where,

K_1= probability factor (risk coefficient)

K_2= terrain, height and structure size factor

K_3= topography factor

V_z= design wind speed at any height z m/s

5.4 Static wind effects

A static force is called as drag force, obstructs an air stream on a bluff body like stack. The distribution of wind pressure depends upon the shape and direction of wind incidence. Due to this a circumferential bending occurs and it is more significant in case of stack having larger diameter. Also drag force creates along-wind shear forces and bending moments.

Drag

The drag force on a single stationary bluff body is :

$$F_d = \frac{1}{2} C_d A \rho U^2 \tag{5.2}$$

Where,

F_d= drag force, N

C_d= Drag coefficient

A = area of section normal to wind direction, sq. m

The value of drag coefficient depends on Reynolds number, shape and aspect ratio of a structure.

Circumferential bending

The radial distribution of wind pressure on horizontal section of the stack depends on Reynolds number. normally the resultant force along wind is counteracted by shear force which is induced in the structure. These shear forces are assumed to vary sinusoidally along the circumference of the stack cell.

Wind load on liners

In both single-flue and multi-flue stack metal liners are being used but these metal liner are not directly exposed to the wind. But they are also designed for wind loads which are transmitted through the stack cell. The magnitude of the force may be found by considering the liner as a beam of varying moment of inertia, acted upon by a transverse load at the top and deflection is calculated at the top of the cell.

5.5 Dynamic wind effects

Wind load is a combination of steady and a fluctuating component. Due to turbulence effect the wind load varies in its magnitude.

Gust loading

Due to fluctuations wind load is random in nature. This load can be expressed as :

$$F(t) = K(U + \varrho) \tag{5.3}$$

$$= K(U^2 + 2U\varrho)$$

Where,

$K = \frac{1}{2} C_d A \varrho$

In the above expression (KU^2) is quasi-static and U is the mean velocity.

Aerodynamic Effects

In wind engineering there is a term called "aerodynamic admittance coefficient" which depends on spatial characteristics of wind turbulence. Spatial characteristics relates to structure's response to wind load, at any frequency. This coefficient is expressed as :

$$A_n = \frac{1}{(1 + \frac{8Hn}{3U_t})(1 + \frac{nD_{co}}{U_t})} \tag{5.4}$$

Where,

A_n= aerodynamic admittance at the structure's natural frequency n, Hz

U_t= mean wind speed at top of a stack, m/s

Always this coefficient has to be multiplied with response of a structure due to wind loads because it allows response modification due to spatial wind-turbulence characteristics.

Vortex formation

When wind is flows through a circular cross section like stack, vortices are formed. These vortices can cause a pressure drop across the stack at regular pressure intervals. Due to this change in pressure, a lateral force perpendicular to wind direction is created.It depends on Reynolds number which has a range such as sub-critical ($R_e < 3X10^5$),ultra-critical ($R_e > 3X10^5$) and super-critical (3X10^5 to 3X 10^6).

Vortex excitation

The alternate shedding of vertices creates a transverse forces called as lift. According to practical design purpose it is divided into two.

1. In sub-critical and ultra-critical R_e range

The frequency of lift force is regular, but magnitude is random. When frequency of vortex shedding is close to natural frequency of a stack (when its motion is near sinusoidal), maximum response is obtained. The exciting force should be taken as :

$$F_L = 1/2\rho AU^2 Sin\omega_t C_L \tag{5.5}$$

The response of the structure depends on the time-average energy input from the vortex shedding forces. In the expression C_L has the time-average value rms value of the lifting force coefficient with a range of frequencies close to the natural frequency ω_o of the structure.

2. In super-critical R_e range

In this range both frequency and magnitude are random in nature. Here structure's response depends on the power input. If we plot power-input density function S'$_l$(St) again non against non-dimensional frequency St, then the power spectrum of the lift-force should be expressed as :

$$S_l = [1/2\rho AU^2\sqrt{C_L^2}].S_l'(S_t) \tag{5.6}$$

According to the (IS-6533 part-2:1989), if period of natural oscillation for the self supported stack exceeds 0.25 seconds, the design wind load should take into consideration

the dynamic effect due to pulsation of thrust caused by the wind velocity in addition to the static wind load. It depends on the fundamental period of vibration of the stack.

5.6 Seismic effects

Due to seismic action, one more load is acted on the stack. It is considered as vulnerable because stack is tall and slender structure. Seismic force is estimated as cyclic in nature for a short period of time. When stack subjected to cyclic loading, the friction with air, friction between the particles of the structure, friction at the junctions of structural elements, yielding of the structural elements decrease the amplitude of motion of a vibrating structure and reduce to normal with corresponding to time. When this friction fully dissipates the structural energy during its motion, the structure is called critically damped.For designing earthquake resistant structures, it is necessary to evaluate the structural response to ground motion and calculate respective shear force, bending moments. Hence ground motion is the important factor for seismic evaluation. To estimate exact future ground motion and its corresponding response of the structure, it depends on soil-structure interaction, structural stiffness, damping etc.For analysis purpose, stack is behaved like a cantilever beam with flexural deformations. Analysis is carried out by following one of the methods according to the IS code provision:

1. Response-spectrum method (first mode)
2. Modal-analysis technique (using response spectrum)
3. Time-history response analysis.

For chimneys which are less than 90m high called as short chimney/stack, response spectrum method is used.

5.6.1 Response-spectrum method

This method consists of three steps such as,

1. Fundamental period
2. Horizontal seismic force
3. Determine design shears and moments

5.6.1.1 Fundamental period

The fundamental period of the free vibration is calculated by eq. 5.7

$$T = C_T \sqrt{\frac{W_t h}{E_s A g}} \tag{5.7}$$

Where,

C_T= coefficient depending on slenderness ratio of the structure

W_t = total weight of the structure including weight of lining and contents above the base

E_s = modulus of elasticity of material of the structural shell

h = height of the structure above the base

A = area of cross-section at the base of the structural shell

g = acceleration due to gravity

Stiffness of the flared chimney is approximately two times the prismatic chimney. Therefore a conservative estimate of natural time period for this self supported steel chimney will be,

$$T_n = \frac{T}{2} \tag{5.8}$$

5.6.1.2 Horizontal seismic force

The horizontal seismic force (A_h) is to be calculated according to IS 1893 (Part 1): 2002 as following eq. 5.9

$$A_h = \frac{\left[\frac{Z}{2}\right]\left[\frac{S_a}{g}\right]}{\left(\frac{R}{I}\right)} \tag{5.9}$$

Where,

Z = zone factor

I = importance factor

R = response reduction factor (The ratio shall not be less than 1.0)

$\frac{S_a}{g}$= spectral acceleration coefficient for rock and soil sites

5.6.1.3 Shear and moment

Base moment and base shear can be calculated as follows :

$$P_{dyn} = \int_0^h dP_{dyn} \tag{5.10}$$

$$M_{dyn} = \int_0^h x dP_{dyn} \tag{5.11}$$

As per IS 6533 (Part-2): 1989 Inertia force, dyn dP , for ith mode for an infinitesimal height dx at a height x from the base of the chimney is as follows:

$$dP_{dyn} = dm.\xi_i.\eta_{|i}.v \tag{5.12}$$

Where,

dm = mass of the chimney for an infinitesimal height dx at height x from the base of the chimney

$\xi_i = \frac{T_i V_b}{1200}$ is the dynamic coefficient for the ith mode of vibration

T_i = the period of ith mode

V_b =basic wind speed in m/s

v = coefficient which takes care of the space

5.7 Temperature effects

The shell of the chimney should withstand the effects of thermal gradient. Due to thermal gradient vertical and circumferential stress are developed and this values estimated by the magnitude of the thermal gradient under steady state condition.

5.8 Analytical design of steel stack as per IS standard

5.8.1 Applicable IS standard code used

5.8.1.1 IS 875 (Part 3), 1987

Code of practice for design loads other than earthquake for buildings and structures (wind loads). This Indian standard IS: 875 (Part-3) was adopted by bureau of Indian Standards after the draft finalized by the structural safety sectional committee had been approved by the civil engineering division council. This part covers,

1. Wind loads to be considered when designing buildings, structures and components.

2. It gives the basic wind speeds for various locations in India.
3. Factors to be considered while estimating the design wind speed/pressure.

5.8.1.2 IS 6533 (Part 1), 1989

Indian standard design and construction of steel stacks-code of practice (Mechanical aspects). This includes,

1. Determination of inside diameter.
2. Determination of stack height based on pollution norms and dispersion of gases into the atmosphere.
3. Estimation of draft losses.
4. General requirements for materials of construction, insulation, lining and cladding.

5.8.1.3 IS 6533 (Part 2), 1989

This is Indian Standard Code of practice for design and construction of steel chimneys (structural aspect). This includes

1. Material of construction for bolts, plates, rivets and welding.
2. General design aspects covering minimum thickness of shell. Allowable stresses, allowable deflection, determination of dynamic force and checking for resonance.
3. Typical ladder details, painters trolley, location of warning lamps and the flue opening details, inspection, maintenance and protective coatings.

5.8.1.4 IS 1893 (Part 4), 2005

This is Indian Standard Code of practice for design of earthquake resistant structure. This includes:

1. Selection of category of the structure.
2. Using code specific spectra, the seismic co-efficient is calculated using this code
3. The fundamental time period for stack is given through this code.

5.8.2 Design methodology

IS:6533 (Part-1 and 2): 1989, IS 875 (Part-3 and 4): 1987, and IS 1893 (Part-4):2005 will be used as the basis for design, which gives detailed procedure to determine static, dynamic and seismic loads coming on the structure.

5.8.2.1 Assumptions

1. The wind pressure varies with the height. It is zero at the ground and increase as the height increases. For the purpose of design it is assumed the wind pressure is uniform throughout the height of the stack.
2. It is assumed that the static wind load (projected area multiplied by the wind pressure) is acting at the center of pressure.
3. In calculating the allowable stresses both tensile and bending, the joint efficiency for butt welds is assumed to be 0.85.
4. The base of the stack is perfectly rigid and the effect of the gussets and stool plate on the deflection and the stresses in the stack is not considered. This is applicable only for manual calculations.
5. There are no additional lateral movements from the duct transferred to the stack; suitable arrangement has to be provided to absorb this movement from the duct.
6. Earthquake causes impulsive ground motions, which are complex and irregular in character, changing in period and amplitude each lasting for a small duration. Therefore resonance of the type as visualized under steady-state sinusoidal excitations will not occur, as it would need time to build up such amplitudes.
7. Earthquake is not likely to occur simultaneously with maximum wind or maximum flood or maximum sea waves.

5.8.3 Analytical design

5.8.3.1 Design input

Flow input to stack : Q_{input} = 97.83 m/s

Basic wind speed : 39 m/s

The temperature to which the stack is expected to be expose : 0 to 150°C

The stack site is located on terrain category 1 and seismic zone III.

Supporting soil condition is medium (Type II).

5.8.3.2 Determination of height

Height as per Gujarat Pollution Control Board for sinter plant :

H = 45 m

5.8.3.3 Other dimensions of stack

1. Height of stack = Ht = 45 m
2. Min. height of flare = h_{flare}= Ht/3 = 15 m (ref. clause 7.2.4; IS-6533 Part-2: 1989)
3. Consider height of flare = h_{flare}= 15 m
4. Height of cylindrical portion of stack =h_{cyl}= Ht- h_{flare}= 30 m
5. Min. outside diameter of unlined stack at top = $d_{top,min}$= h_{cyl}/20 = 30/20 = 1.5 m (ref. Clause 7.24; I S-6533 Part-2:1989)
6. Flow of gas entering = Q = 97.83 m^3/s
7. Velocity of flue gases at exit pt. of stack = V_{02}= 20 m/s
8. Inside diameter of stack = D = $\sqrt{\frac{4Q}{\Pi\ V_{02}}}$ = 2.49 m (ref. clause 6.2; IS-6533 Part-1:1989)
9. Consider outside diameter of the stack at top = d_{top}= 2.5 m
10. Min. outside diameter of flare stack at base = $d_{base,\ min}$= 1.6 d_{top}= 4 m
11. Consider outside diameter of stack at base = d_{base}= 4 m
12. Min. thickness of the shell = T_{min}= d_{top}/500 = 5 mm
13. Consider a shell thickness = $T_{top\ A}$= 6 mm
14. External corrosion allowance = T_{ce}= 3 mm (Ref. Table-1; IS-6533 part-2:1989 for non-copper bearing steel and design life 20 years)
15. Internal corrosion allowance = T_{ci}= 5 mm (Ref. Table-1; IS-6533 part-2:1989 for non-copper bearing steel and design life 20 years)
16. T_{top}= $T_{top\ A}$+ T_{ce}+ T_{ci} = 14 mm

5.8.3.4 Various load combination

1. Dead load + Wind load
2. Dead load + Earthquake load
3. Dead load + Load due to lining + Impose load on service platforms + Wind load
4. Dead load + Load due to lining + Impose load on service platforms + Earthquake load

5.8.3.5 Permissible stress

1. Material consider = IS 2062 : 2006
2. Yield stress of shell = f_y= 250 MPa
3. permissible stress in tension = $f_{allow\ tension}$= 0.6 f_y= 150 MPa (Ref: IS-800: 1984; Clause: 4.11)
4. Efficiency of butt weld = 0.85
5. Allowable tensile stress = $f_{allow\ T}$= Butt weld efficiency . $f_{allow\ tension}$ = 127.5 MPa
6. Max. permissible stress in shear = $f_{allow\ sh}$= 0.4 f_y= 100 MPa (For un-stiffen web as per Ref:-IS-800:1984; Clause: 6.4.2)

5.8.3.6 Stack weight

1. Mass density of the construction material used in stack design = den = 78.5 kN/m^3

Weight of the (platform + access ladder + helical stair + rain cap + etc.) is assumed to be 20% of self weight of stack shell.

5.8.3.7 Wind load calculation

Considering general structure for design life for 50 years.

K_1= 1 (ref. clause 5.3.1; IS-875 Part-3:1987)

K_3= 1 (ref. clause 5.3.1; IS-875 Part-3:1987)

As the chimney site is located on Terrain category 1 is considered for the wind load calculation as per clauses 5.3.2.1, IS-875 (Part-3):1987

As the chimney is 45m tall, the size class of the structure is considered as Class-B as per clause 5.3.2.2, IS-873(part-3):1987

V_b= 39 m/s

Wind load on the chimney will be increased due to the presence of platform, ladder, and other fittings.5% of the wind force on the chimney shell is considered in excess to account this.

5.8.3.8 Design for static wind

For finding wind loads and design of stack the total height of the is divided into 4 parts:35m to 45m,25m to 35m,15m to 25m, and 0 to 15m.

Part 1

It is located at a height of 35 to 45 m from the ground.Considering K_2factor in this height range as per IS 873 (Part 3), 1987, lateral wind force given as :

$P_1 = 0.6V_z^2$

$P_1 = \int_{35}^{45} 0.6[K_1[1.13 + \frac{(h-30)(1.18-1.13)}{(50-30)}]K_3.V_b]^2.d_{top}dh$

= 30.436 kN

Moment due to wind force at the base of part 1:

$M_1 = \int_{35}^{45} 0.6[K_1[1.13 + \frac{(h-30)(1.18-1.13)}{(50-30)}]K_3.V_b]^2.d_{top}.(h-25)dh$

= 457.652 kNm

Section modulus (Z_1) of the stack at 35m level :

$Z_1 = \frac{\pi d_{top}^2 T_{topA}}{4}$

= 0.029 m^3

Bending stress at the extreme fibre of the stack shell at 35m level :

$f_{mo1} = \frac{1.05M_1}{Z_1}$

= 16.570 MPa

Axial compression stress due to self weight of the stack shell :

$f_{st1} = \frac{\int_{35}^{45}(\pi d_{top}.T_{top}).den.dh}{(\pi d_{top}.T_{topA})}$

= 2.289MPa

Axial compression stress due to platform :

$f_{pl1} = 0.2f_{st1} = 0.4578$ MPa

Max. compressive stress :

$f_{c1} = f_{mo1} + f_{st1} + f_{pl1}$

= 19.316 MPa

Max. permissible stress at 35 m level :

$h_{level} = Ht - 35 = 10m$

$\frac{h_{level}}{d_{top}} = 4$ (i.e < 20)

$\frac{d_{top}}{T_{topA}} = 416.66$

Maximum permissible compressive stress at 35m level as per clause 7.7 of IS 6533(Part 2), 1989 (as per the input the temperature to which the chimney shell is expected to be exposed is limited to $0 - 150^oC$) :

$f_{allowc1} = 64 + \frac{(70-64)(450-(\frac{d_{top}}{T_{topA}})}{(450-400)} = 68.0$ MPa (therefore safe , $f_{c1} < f_{allowc1}$)

(Ref.Table-3, IS 6533 Part-2:1989)

Maximum shear stress :

$f_{sh1} = \frac{1.05P_1}{\pi d_{top} T_{topA}} = 0.678$ MPa (therefore safe , $f_{sh1} < f_{allowsh}$)

Part 2

It is located at a height of 25 to 35m from the ground. Considering K_2factor in this height range as per IS 873 (Part 3), 1987, lateral wind force given as :

$P_{2a} = \int_{30}^{35} 0.6[K_1[1.13 + \frac{(h-30)(1.18-1.13)}{(50-30)}]K_3.V_b]^2.d_{top}dh$

= 14.727kN

$P_{2b} = \int_{25}^{30} 0.6[K_1[1.10 + \frac{(h-20)(1.13-1.10)}{(30-20)}]K_3.V_b]^2.d_{top}dh$

= 14.373 kN

Shear force due to wind force at base of part 2 :

$P_2 = P_1 + P_{2a} + P_{2b} = 59.536$ MPa

Moment due to wind force at base of part 2 :

$M_{2a} = \int_{25}^{30} 0.6[K_1[1.10 + \frac{(h-20)(1.13-1.10)}{(30-20)}]K_3.V_b]^2.d_{top}.(h-25)dh$

= 36.094 kNm

$M_{2b} = \int_{30}^{45} 0.6[K_1[1.13 + \frac{(h-30)(1.18-1.13)}{(50-30)}]K_3.V_b]^2.d_{top}.(h-25)dh$

= 560.851 kNm

$M_2 = M_{2a} + M_{2b} = 596.851$ kNm

Considering an improved wall thickness for this part :

$T_{2A} = T_{topA} + 2mm = 8mm$

Therefore overall wall thickness of shell including the corrosion allowances :

$T_2 = T_{2A} + T_{ce} + T_{ci} = 16mm$

Section modulus (Z_2) of tubular stack section at 25m level :

$Z_2 = \frac{\pi d_{top}^2 . T_{2A}}{4} = 0.03m^3$

Bending stress at the extreme fiber of the stack shell at 25m level :

$f_{mo2} = \frac{1.05 M_2}{Z_2} = 16.069$ MPa

Axial compression stress due to self weight of the stack shell :

$f_{st2} = \frac{\int_{35}^{45} (\pi d_{top} . T_{top}) . den . dh + \int_{30}^{35} (\pi d_{top} . T_{top}) . den . dh}{(\pi d_{top} . T_{top2A})}$

$= 2.472$ MPa

Axial compression stress due to platform :

$f_{pl2} = 0.2 f_{st2} = 0.4944$ MPa

Max. tensile stress :

$f_{t2} = f_{mo2} = 16.069$ MPa

Max. compressive stress :

$f_{c2} = f_{mo2} + f_{st2} + f_{pl2}$

$= 19.035$ MPa

Max. permissible stress at 25m level :

$h_{level2} = Ht - 25 = 20m$

$\frac{h_{level2}}{d_{top}} = 8$ (i.e < 20)

$\frac{d_{top}}{T_{2A}} = 312.5$

Maximum permissible compressive stress at 25m level as per clause 7.7 of IS 6533(Part 2), 1989 (as per the input the temperature to which the chimney shell is expected to be exposed is limited to $0 - 150^oC$) :

$f_{allowc2} = 78 + \frac{(87-78)(450-(\frac{d_{top}}{T_{topA}})}{(350-300)} = 84.075$ MPa (therefore safe , $f_{c1} < f_{allowc1}$)

(Ref.Table-3, IS 6533 Part-2:1989)

Maximum shear stress :

$f_{sh2} = \frac{1.05 P_2}{\pi d_{top} . T_{2A}} = 0.994$ MPa (therefore safe , $f_{sh1} < f_{allowsh}$)

Part 3

It is at height 15 to 25m from ground.Considering K_2factor in this height range as per IS 873 (Part 3), 1987, lateral wind force given as :

$P_{3a} = \int_{20}^{25} 0.6[K_1[1.10 + \frac{(h-20)(1.13-1.10)}{(30-20)}]K_3 V_b]^2 . d_{top} dh$

$= 13.99$kN

$P_{3b} = \int_{15}^{20} 0.6[K_1[1.07 + \frac{(h-15)(1.10-1.07)}{(20-15)}]K_3V_b]^2.d_{top}dh$

$= 13.43$ kN

Shear force due to wind force at base of part 3 :

$P_3 = P_2 + P_{3a} + P_{3b} = 86.956$ MPa

Moment due to wind force at base of part 3 :

$M_{3a} = \int_{15}^{20} 0.6[K_1.[1.07 + \frac{(h-15)(1.10-1.07)}{(20-15)}].K_3.V_b]^2.d_{top}.(h-15)dh$

$= 33.88$ kNm

$M_{3b} = \int_{20}^{30} 0.6[K_1.[1.10 + \frac{(h-20)(1.13-1.10)}{(30-20)}].K_3.V_b]^2 d_{top}.(h-15)dh$

$= 284.93$ kNm

$M_{3c} = \int_{30}^{45} 0.6[K_1.[1.13 + \frac{(h-30)(1.18-1.13)}{(50-30)}].K_3.V_b]^2 d_{top}.(h-15)dh$

$= 1019.89$ kNm

$M_3 = M_{3a} + M_{3b} + M_{3c} = 1338.66$ kNm

Considering an improved wall thickness for this part :

$T_{3A} = T_{2A} + 2mm = 10mm$

Therefore overall wall thickness of shell including the corrosion allowances :

$T_2 = T_{2A} + T_{ce} + T_{ci} = 18mm$

Section modulus (Z_3) of tubular stack section at 15m level :

$Z_3 = \frac{\pi d_{top}^2.T_{3A}}{4} = 0.049m^3$

Bending stress at the extreme fiber of the stack shell at 15m level :

$f_{mo3} = \frac{1.05M_3}{Z_3} = 28.685$ MPa

Axial compression stress due to self weight of the stack shell :

$f_{st3} = \frac{\int_{35}^{45}(\pi d_{top}.T_{top}).den.dh + \int_{25}^{35}(\pi d_{top}.T_{top}).den.dh + \int_{15}^{25}(\pi d_{top}.T_{top}).den.dh}{(\pi d_{top}.T_{top3A})}$

$= 30.772$ MPa

Axial compression stress due to platform :

$f_{pl3} = 0.2f_{st3} = 6.154$ MPa

Max. tensile stress :

$f_{t3} = f_{mo3} = 28.685$ MPa

Max. compressive stress :

$f_{c3} = f_{mo3} + f_{st3} + f_{pl3}$

$= 65.611$ MPa

Max. permissible stress at 15m level :

$h_{level3} = Ht - 15 = 30m$

$\frac{h_{level3}}{d_{top}} = 12$ (i.e < 20)

$\frac{d_{top}}{T_{3A}} = 250$

Maximum permissible compressive stress at 15m level as per clause 7.7 of IS 6533(Part 2), 1989 (as per the input the temperature to which the chimney shell is expected to be exposed is limited to $0 - 150^oC$) :

$f_{allowc3} = 90$ MPa (therefore safe , $f_{c3} < f_{allowc3}$)

Maximum shear stress :

$f_{sh23} = \frac{1.05P_3}{\pi d_{top}.T_{3A}} = 1.162$ MPa (therefore safe , $f_{sh3} < f_{allowsh}$)

Part 4

It is at height 0 to 15m from ground.Considering K_2factor in this height range as per IS 873 (Part 3), 1987, lateral wind force given as :

$P_{4a} = \int_0^{10} 0.6[K_1.(1.03).K_3.V_b]^2.[d_{base} - [\frac{h.(d_{base}-d_{top})}{h_{flare}}]]dh$

$= 33.88$kN

$P_{4b} = \int_{10}^{15} 0.6[K_1.[1.03 + \frac{(h-10)(1.07-1.03)}{(15-10)}].K_3.V_b]^2.[d_{base} - [\frac{h(d_{base}-d_{top})}{h_{flare}}]]dh$

$= 13.820$ kN

Shear force due to wind force at base of part 4 :

$P_4 = P_3 + P_{4a} + P_{4b} = 134.656$ MPa

Moment due to wind force at base of part 4 :

$M_{4a} = \int_0^{10} 0.6[K_1.(1.03).K_3V_b]^2.[d_{base} - [\frac{h(d_{base}-d_{top})}{h_{flare}}]] * hdh$

$= 161.362$kN

$M_{4b} = \int_{10}^{15} 0.6[K_1.[1.03 + \frac{(h-10)(1.07-1.03)}{(15-10)}].K_3.V_b]^2.[d_{base} - [\frac{h(d_{base}-d_{top})}{h_{flare}}]].hdh$

$= 172.142$ kNm

$M_{4c} = \int_{15}^{20} 0.6[K_1.[1.07 + \frac{(h-15)(1.10-1.07)}{(20-15)}].K_3.V_b]^2.d_{top}hdh$

$= 235.33$ kNm

$M_{4d} = \int_{20}^{30} 0.6[K_1.[1.10 + \frac{(h-20)(1.13-1.10)}{(30-20)}].K_3.V_b]^2.d_{top}hdh$

$= 710.419$ kNm

$M_{4e} = \int_{30}^{45} 0.6[K_1.[1.13 + \frac{(h-30)(1.18-1.13)}{(50-30)}].K_3.V_b]^2.d_{top}hdh$

= 1697.370 kNm

$M_4 = M_{4a} + M_{4b} + M_{4c} + M_{4d} + M_{4e} = 2976.61$ kNm

Considering an improved wall thickness for this part :

$T_{4A} = T_{3A} + 2mm = 12mm$

Therefore overall wall thickness of shell including the corrosion allowances :

$T_4 = T_{4A} + T_{ce} + T_{ci} = 20mm$

Section modulus (Z_3) of tubular stack section at base :

$Z_4 = \frac{\pi d_{top}^2 T_{4A}}{4} = 0.058m^3$

Bending stress at the extreme fibre of the stack shell at base :

$f_{mo4} = \frac{1.05M_4}{Z_4} = 53.886$ MPa

Axial compression stress due to self weight of the stack shell :

$f_{st4} = \frac{\int_{35}^{45}(\pi d_{top}.T_{top}).den.dh + \int_{25}^{35}(\pi d_{top}.T_{top}).den.dh + \int_{15}^{25}(\pi d_{top}.T_{top}).den.dh + \int_{0}^{15}(\pi d_{top}.T_{top}).den.dh}{(\pi d_{top} T_{top4A})}$

= 0.066 MPa

Axial compression stress due to platform :

$f_{pl4} = 0.2 f_{st4} = 0.0132$ MPa

Max. tensile stress :

$f_{t4} = f_{mo4} = 53.886$ MPa

Max. compressive stress :

$f_{c4} = f_{mo4} + f_{st4} + f_{pl4}$

= 53.965 MPa

Max. permissible stress at base :

$h_{level4} = Ht - 0 = 45m$

$d_{level4} = \frac{d_{top} + d_{base}}{2} = 3.25m$

$\frac{h_{level4}}{d_{level4}} = 13.84$ (i.e < 20)

$\frac{d_{top}}{T_{4A}} = 333.33$

Maximum permissible compressive stress at base as per clause 7.7 of IS 6533(Part 2), 1989 (as per the input the temperature to which the chimney shell is expected to be exposed is limited to $0 - 150^oC$) :

$f_{allowc4} = 78 + \frac{(87-78)(450-(\frac{d_{top}}{T_{topA}})}{(350-300)} = 81.000$ MPa (therefore safe , $f_{c4} < f_{allowc4}$)

(Ref.Table-3, IS 6533 Part-2:1989)

Maximum shear stress :

$f_{sh24} = \frac{1.05P_4}{\pi d_{top}.T_{4A}} = 1.50$ MPa (therefore safe , $f_{sh4} < f_{allowsh}$)

5.8.3.9 Check for seismic force

Area of cross-section at the base of stack shell :

$A_{base} = \pi d_{base}.T_3 = 0.226m^2$

Radius of gyration of the structural shell at the base section :

$r_e = \frac{1}{\sqrt{2}}.(\frac{d_{base}}{2}) = 1.41m$

Slenderness ratio :

$k = \frac{Ht}{r_e} = 31.91$

Coefficient depending upon slenderness ratio :

$C_T = 56$

(ref. clause 14.1 and Table-6; IS-1893 Part-4:2005)

Weight of the stack :

$W_s = \int_{35}^{45}(\pi d_{top}.T_{top}).den.dh + \int_{25}^{35}(\pi d_{top}.T_2).den.dh + \int_{15}^{25}(\pi d_{top}.T_3).den.dh + \int_{0}^{15}\pi(\frac{d_{base}+d_{top}}{2}).T_4.den.dh$

$= 536.38kN$

Weight of platform,ladder etc :

$W_p = 0.2W_s = 107.276kN$

Total weight of the stack :

$W_T = W_s + W_p = 643.65kN$

Modulus of elasticity of material :

$E_s = 200000$ MPa

The fundamental period of vibration (ref. clause 14.1; IS-1893 Part-4:2005): :

$T_n = C_T\sqrt{\frac{W_T.Ht}{E_s.A_{base}.g}} = 0.226$s

Stiffness of the flare stack is approximately two times the prismatic stack. Therefore the conservative estimate of natural time period for this stack will be :

$T_{n,emperical} = \frac{T_n}{2} = 0.1131s$

$S_a = 1.4(2.5g) = 3.5$g

Importance factor for steel stack :

$I = 1.5$ (ref. table-8, IS 1893 Part-4:2005)

Response reduction factor :

$R_f = 2$ (ref. table-9, IS 1893 Part-4:2005)

Zone factor :

$Z = 0.10$ (ref. table-2, IS 1893 Part-1:2002 for zone ii)

Design horizontal acceleration spectrum value :

$A_h = \frac{(\frac{Z}{2}).(\frac{S_a}{g})}{(\frac{R_f}{I})} = 0.131$

Design of base shear :

$V_B = A_h.W_T = 84.31kN$

Calculation for design moment :

Denominator$_1$= $\int_{35}^{45} \pi d_{top}.T_{top}.den.h^2 dh = 138823.70kNm$

Denominator$_2$= $\int_{25}^{35} \pi d_{top}.T_2.den.h^2 dh = 89603.45$kNm

Denominator$_3$= $\int_{15}^{25} \pi d_{top}.T_3.den.h^2 dh = 45315.51kNm$

Denominator$_4$= $\int_{0}^{15} \pi[d_{base} - \frac{(d_{base}-d_{top}).h}{(15-0)}].T_4.den.h^2 dh = 15952.90kNm$

Denominator = Denominator$_1$+ Denominator$_2$ + Denominator$_3$ + Denominator$_4$= 164695.56 kNm

Moment due to seismic force :

$M_{s1} = \frac{\int_{35}^{45} \pi.d_{top}.T_{top}.den.h^2.V_B.(h-35)dh}{Denominator} = 177.99kNm$

$f_{smo1} = \frac{1.05M_{s1}}{Z_1} = 6.4MPa$

$f_{sc1} = f_{smo1} + f_{st1} + f_{pl1} = 9.146MPa$ therefore safe

Moment due to seismic force at the 25m level :

Numerator$_{2a}$= $\int_{35}^{45} \pi.d_{top}.T_{top}.den.h^2.V_B.(h-25)dh = 83456065kNm$

Numerator$_{2b}$= $\int_{25}^{35} \pi.d_{top}.T_2.den.h^2.V_B.(h-25)dh = 19396271.58kNm$

$M_{s2} = \frac{Numerator_{2a}+Numerator_{2b}}{Denominator} = 624.49kNm$

$f_{smo2} = \frac{1.05M_{s2}}{Z_2} = 21.857MPa$

$f_{sc2} = f_{smo2} + f_{st2} + f_{pl2} = 24.863MPa$ therefore safe

Moment due to seismic force at the 15m level :

Numerator$_{3a}$= $\int_{35}^{45} \pi.d_{top}.T_{top}.den.h^2.V_B.(h-15)dh = 137597310.9kNm$

Numerator$_{3b}$= $\int_{25}^{35} \pi.d_{top}.T_2.den.h^2.V_B.(h-15)dh = 54341620.39kNm$

Numerator$_{3c}$= $\int_{15}^{25} \pi.d_{top}.T_3.den.h^2.V_B.(h-15)dh = 10279222.44kNm$

$M_{s3} = \frac{Numerator_{3a}+Numerator_{3b}+Numerator_{3c}}{Denominator} = 1227.83kNm$

$f_{smo3} = \frac{1.05M_{s3}}{Z_3} = 26.310MPa$

$f_{sc3} = f_{smo3} + f_{st3} + f_{pl3} = 63.236MPa$ therefore safe

Moment due to seismic force at the 0m level :

$\text{Numerator}_{4a} = \int_{35}^{45} \pi.d_{top}.T_{top}.den.h^2.V_B.hdh = 218809179.4kNm$

$\text{Numerator}_{4b} = \int_{25}^{35} \pi.d_{top}.T_2.den.h^2.V_B.hdh = 106759643.6kNm$

$\text{Numerator}_{4c} = \int_{15}^{25} \pi.d_{top}.T_3.den.h^2.V_B.hdh = 36788796.1kNm$

$\text{Numerator}_{4d} = \int_{0}^{15} \pi[d_{base} - \frac{(d_{base}-d_{top}).h}{(15-0)}].T_4.den.h^2.V_B.hdh = 6816747.51kNm$

$M_{s4} = \frac{Numerator_{4a}+Numerator_{4b}+Numerator_{4c}+Numerator_{4d}}{Denominator} = 2241.55kNm$

$f_{smo4} = \frac{1.05M_{s4}}{Z_4} = 40.579MPa$

$f_{sc4} = f_{smo4} + f_{st4} + f_{pl4} = 40.649MPa$ therefore safe

In case of self-supporting stack, if the time period of natural oscillation for the stack computed exceeds 0.25sec, the design wind load shall take ino consideration the dynamic effect due to the pulsating of the thrust caused by wind velocity in addition to the static wind load.

5.8.3.10 Check for resonance

Fundamental period of vibration for stack :

$T_{emperical} = 0.1131sec$

Fundamental frequency of vibration :

$f = \frac{1}{T_{emperical}} = 8.84Hz$

Stroughal critical velocity :

$V_{cr} = 5d_{top}f = 110.5$m/s (ref. clause A-3, IS-6533 Part-2:1989)

Basic wind velocity = V_b= 39m/s

Design wind velocity = V_d= K_1. K_3. (1.15) . V_b= 44.85m/s

Velocity (Stroughal critical velocity) range for resonance :

$V_{resonan_{ul}} = 0.8V_d = 35.88m/s$

$V_{resonan_{ll}} = 0.33V_d = 14.80m/s$

As the Stroughal critical velocity is not lies within the range of resonance limits , the stack does't required to check for resonance.Therefore stack is safe.

Chapter 6

Conclusion & future scope

The various components like ducting network, cyclonic separator and stack of de-dusting system for sinter plant have been designed and following points are concluded.

6.1 Conclusion

1. The desired flow inside ducts network is depends upon different losses associated with the duct. The pressure drop increases in direction of flow.
2. The equal pressure drop has been achieved inside duct network to obtain desired flow.
3. The safe design of duct is carried out according to ASME B31.3 and BPV section VIII division I.
4. In cyclonic separator design has been carried out with different available mathematical models. The collection efficiency increases as height of cyclonic separator increases and size of dust particle increases.
5. The design of self supporting steel stack is carried out according IS:6533 (Part 1 and 2) standard.

6.2 Future scope

1. The verification of design of steel stack can be done through STADD Pro software.
2. The stress generated at different portion of stack can be determined by considering manhole of standard size.

References

[1] American Conference of Governmental Industrial Hygienists, General introduction of de-dusting systems (ACGIH), 1988.

[2] American Society of Heating, Refrigeration and Air conditioning Engineers, Chapter 35 Duct design, 2005.

[3] American Society of Mechanical Engineers (ASME) B31.3: Process Piping, Design of external pressurized pipes, 2010.

[4] American Society of Mechanical Engineers (ASME) B31.1: Pressure Piping, Selection of span for pipe, 2007.

[5] American Society of Mechanical Engineers (ASME) for BPV- Section VIII and Division I, Design of external pressurized pipes, 2013.

[6] Dr.D.P Vakharia andMr Mohd. Farooq A, Determination of span between pipes supports using maximum bending theory, International Journal of Recent Trends in Engineering, Vol.1, May 2009.

[7] US Army Corps of Engineers, Liquid process piping, May 1999.M.Heeumann, JR

[8] ESSAR Piping stress analysis notes, Piping stress analysis.

[9] Z.W. Ma, P. Zhang,Pressure drops and loss coefficients of a phase change material slurry in pipe fittings, 2102.

[10] P.L. Spedding , E. Benard, G.F. Donnelly,Prediction of pressure drop in multiphase horizontal pipe flow,Sep 2006.

[11] Daniel Vasilikis,SpyrosA.Karamanos,Stability of confined thin-walled steel cylinders under external pressure, 2009.

[12] A. Buckshumiyan, AR. Veerappan, S. Shanmugam,Determination of collapse loads in pipe bends with ovality and variable wall thickness under internal pressure and in-plane opening moment.

[13] M.Heeumann, JR., Understanding cyclone dust collector, Plant engineering, May 26, 1983.

[14] Cyclonic separator, NPTEL module 5, Chemical engineering design.

[15] EPC Industrial manual edition 2, 2002

[16] Lingjuan Wang, Theoretical study of cyclonic separator, Phd dissertation from Texas A and M University, May 2004.

[17] Bureau of Indian Standard, Indian Standard (IS:6533,Part-1)- Design and construction of steel chimney-code of practice,2002.

[18] Bureau of Indian Standard, Indian Standard (IS:6533, Part-2)- Design and construction of steel chimney,2002.

[19] Bureau of Indian Standard, Indian Standard (IS:1893)-Criteria for earth quake resistant design of structure,2002.

[20] Bureau of Indian Standard, Indian Standard (IS:875, Part 3), Wind Load on Building and Structure,2002.

[21] Kirtikant Shaoo,Analysis of self supporting steel chimney as per Indian standard, M.Tech dissertation from NIT Rourkela, May 2012.

Appendix

A1.1 Friction loss calculation

The friction loss of different ducts is given in table 6.16.26.3

Table 6.1: Friction loss in different ducts

Branch	Di (mm)	L (m)	V (m/s)	Re	A	B	f	ΔP_f(Pa)
1-a	260.35	5	24.757	427980.2007	4.64189E+21	1.22258E-17	0.015658999	110.5919990
2-a	206.38	7	25.845	354170.369	3.25042E+21	2.52733E-16	0.016372251	222.5579662
3-b	339.75	4.5	27.747	625955.6718	7.7892E+21	2.78843E-20	0.014677915	89.8050426
4-e	260.35	5.5	22.846	394944.285	4.36063E+21	4.42063E-17	0.015781822	104.4080168
5-e	339.75	6	26.966	608336.7804	7.63186E+21	4.40303E-20	0.014715401	113.3830697
6-j	260.35	5	26.764	462675.6914	4.92033E+21	3.51261E-18	0.015545387	128.3119944
7-j	260.35	5	27.517	475692.9831	5.02059E+21	2.25335E-18	0.015506238	135.2920517
8-j	260.35	5	24.824	429138.4458	4.65145E+21	1.17084E-17	0.015654969	111.1627848
9-c	260.35	7.5	23.882	412853.8657	4.51513E+21	2.17428E-17	0.015713285	154.9042360
10-h	206.38	6	26.136	358158.126	3.27792E+21	2.11281E-16	0.016355014	194.8785581
11-h	339.75	3	26.845	605607.093	7.60716E+21	4.73153E-20	0.014721366	56.2066839
12-i	260.35	7	27.028	467239.5227	4.95574E+21	3.00209E-18	0.015531461	183.0340274
13-i	260.35	9	25.238	436295.3631	4.71015E+21	8.98602E-18	0.01563045	206.4987978
14-p	1200	10	23.767	1893754.56	4.69341E+22	5.6608E-28	0.011726414	33.1195144
15-o	787.6	5	26.929	1408296.219	2.78364E+22	6.47072E-26	0.0125177	34.5764603
16-u	260.35	5	24.73	427513.4452	4.63803E+21	1.24412E-17	0.015660628	110.3623866
17-x	206.38	5	25.467	348990.3961	3.21433E+21	3.1992E-16	0.016395115	154.5694608
18-x	339.75	5	23.986	541109.7684	6.9967E+21	2.86742E-19	0.014876107	75.5730117
19-gg	206.38	5	25.632	351251.4954	3.23013E+21	2.88513E-16	0.016385068	156.4828954
20-gg	339.75	5	22.79	514128.726	6.72517E+21	6.49991E-19	0.014949891	68.5627860
21-hh	260.35	5	24.541	424246.1568	4.61091E+21	1.4066E-17	0.015672111	108.7616252
22-aa	206.38	5	27.423	375794.7003	3.39678E+21	9.79144E-17	0.016282359	177.9921691
23-z	339.75	5	25.238	569354.1372	7.27051E+21	1.27039E-19	0.014804894	83.2677784
24-z	260.35	5	25.05	433045.362	4.68359E+21	1.0128E-17	0.015641504	113.0987051
25-dd	206.38	6	27.15	372053.6088	3.37194E+21	1.14913E-16	0.016297303	209.5512698
26-dd	339.75	4	27.631	623338.7814	7.76606E+21	2.98175E-20	0.014683374	79.1900932
27-bb	206.38	5	26.148	358322.5695	3.27905E+21	2.09735E-16	0.01635431	162.5409611
28-bb	339.75	5	24.064	542869.4016	7.01406E+21	2.72227E-19	0.014871498	76.0417571

Table 6.2: Friction loss in different ducts

Branch	Di (mm)	L (m)	V (m/s)	Re	A	B	f	ΔP_f(Pa)
29-cc	260.35	8	21.773	376395.0765	4.19534E+21	9.54452E-17	0.015858235	138.6037727
30-ee	206.38	3	26.634	364982.5347	3.32445E+21	1.56208E-16	0.016326226	101.0097934
31-ff	339.75	5	27.266	615104.6004	7.69273E+21	3.6887E-20	0.014700798	96.5040514
32-m	260.35	5	31.473	544081.3045	5.51289E+21	2.62686E-19	0.015325987	174.9316539
33-s	206.38	5	27.885	382125.7783	3.43837E+21	7.49472E-17	0.016257612	183.7603033
34-s	339.35	5	25.814	581662.7318	7.37905E+21	9.0223E-20	0.014777496	87.0532231
35-t	260.35	5	23.204	401133.117	4.41458E+21	3.447E-17	0.015757586	97.7640264
36-v	206.38	5	27.963	383194.6616	3.44533E+21	7.16714E-17	0.0162535	184.7430284
37-v	339.75	5	22.945	517625.433	6.76092E+21	5.83186E-19	0.014939985	69.4525293
38-y	206.38	5	26.709	366010.3071	3.3314E+21	1.49336E-16	0.016321966	169.2549422
39-y	339.75	5	25.138	567098.1972	7.24902E+21	1.35371E-19	0.014810374	82.6397982
a-b	339.75	1	24.16	545035.104	7.03538E+21	2.55426E-19	0.014865858	15.32412326
b-c	495.3	1.5	24.52	806411.7984	1.29016E+22	4.84336E-22	0.013780683	15.05517624
c-d	590.94	6.5	24.14	947215.3622	1.67256E+22	3.68873E-23	0.013340695	51.30671417
e-d	441.16	6	27.96	819032.951	1.18435E+22	3.77777E-22	0.013928869	88.8580084
d-f	688.6	5	26.01	1189256.27	2.22445E+22	9.67497E-25	0.012873548	37.9431338
h-f	390.56	7.5	27.68	717830.5331	9.70984E+21	3.11678E-21	0.014279055	126.053928
f-g	787.6	1	26.72	1397366.221	2.7686E+22	7.32982E-26	0.012526179	6.812979037
i-g	390.56	6	23.33	605021.1827	8.55984E+21	4.80538E-20	0.014505836	72.77579778
g-l	889.6	12	25.5	1506270.72	3.20451E+22	2.20602E-26	0.01229932	64.72904394
k-l	495.3	5	22.25	731756.22	1.19836E+22	2.29189E-21	0.013908418	41.70524563
j-k	390.56	5	24.2	627583.0528	8.80211E+21	2.67496E-20	0.014455316	65.02671401
l-p	1000	60	25.68	1705152	3.81782E+22	3.03283E-27	0.012033012	285.6714847
p-q	1600	5	23.62	2509388.8	7.00236E+22	6.2657E-30	0.01115439	11.66828112
v-t	390.56	5	25.22	654034.9005	9.07808E+21	1.38179E-20	0.014399642	70.35182325
t-r	495.3	5	22.18	729454.0656	1.19542E+22	2.4104E-21	0.013912682	41.45594874
r-n	650	5	22.86	986637.6	1.85522E+22	1.92103E-23	0.013168967	31.7623073
n-m	900	5	23.86	1425873.6	3.10706E+22	5.30592E-26	0.012346889	23.43026365
u-n	650	5	22.85	986206	1.85461E+22	1.93453E-23	0.013169512	31.7358401
w-u	590.94	5	22.78	893851.1165	1.6012E+22	9.32855E-23	0.013413606	35.33709604
x-w	390.56	5	25.36	657665.5462	9.1153E+21	1.26467E-20	0.01439228	71.09868943
y-w	390.56	5	26.67	691638.0173	9.45605E+21	5.64931E-21	0.014326406	78.27386446
dd-ee	390.56	1	28.65	742985.7216	9.94659E+21	1.79626E-21	0.014236122	17.95165299
ee-ff	488.94	4	23.02	747358.4803	1.20579E+22	1.63529E-21	0.013897678	36.15002019
ff-kk	500	5	24.97	829004	1.32686E+22	3.1128E-22	0.013732446	51.3731537
bb-cc	390.56	3	25.58	663370.8467	9.17346E+21	1.10142E-20	0.014380841	43.36807247
cc-ii	488.94	5	22.61	734047.5778	1.18924E+22	2.18007E-21	0.013921703	43.6675865
z-aa	441.16	5	23.84	698345.6922	1.05472E+22	4.84094E-21	0.014132177	54.61937314
aa-jj	488.94	5	24.32	789563.7811	1.25689E+22	6.78987E-22	0.013825762	50.1743661
gg-hh	390.56	12	24.48	634844.3443	8.87873E+21	2.22526E-20	0.014439666	159.5235098

Table 6.3: Friction loss in different ducts

Branch	Di (mm)	L (m)	V (m/s)	Re	A	B	f	ΔP_f(Pa)
hh-ii	495.3	11	22.12	727480.7904	1.1929E+22	2.51717E-21	0.013916353	90.7342596
ii-jj	700	9	22.18	1030926.4	2.02709E+22	9.51512E-24	0.013023932	49.42662134
jj-kk	848.16	5	23.23	1308263.052	2.79235E+22	2.10347E-25	0.012512816	23.88344285
kk-20	488.94	16	23.09	749631.0734	1.20859E+22	1.55774E-21	0.013893643	145.4385925
m-o	950	5	23.81	1501934.8	3.35701E+22	2.31015E-26	0.012228051	21.89140766
i-g	390.56	5	23.4	606836.5056	8.57957E+21	4.58047E-20	0.014501661	60.99341591
o-q	1250	5	24.6	2041800	5.09828E+22	1.69764E-28	0.011605755	16.85601288
s-r	390.56	5	27.51	713421.8918	9.66765E+21	3.43965E-21	0.014286829	83.05208189
q-20	2000	25	24.75	3286800	9.8339E+22	8.34996E-32	0.010690813	2.046497268

A1.2 Dynamic loss calculation

The Dynamic loss is calculated and given in table 6.46.5

Table 6.4: Dynamic loss in different ducts

Branch	V (m/s)	No.$_{45}$	K$_{45}$	No.$_{90}$	K$_{90}$	K$_b$	K$_a$	K$_d$	K	P$_v$	ΔP$_j$(Pa)
1-a	24.75	1	0.1007	2	0.201	0.402	-0.03	0.9	1.344	367.75	494.07
2-a	25.84	0	0	2	0.218	0.437	0.54		0.978	400.78	391.76
3-b	27.74	0	0	1	0.167	0.167	0.48	0.9	1.518	461.94	700.99
4-e	22.84	0	0	2	0.201	0.402	0.61		1.013	313.16	317.17
5-e	26.96	0	0.083	1	0.167	0.167	-0.24	0.8	0.714	436.30	311.41
6-j	26.76	1	0.100	2	0.201	0.402	0.48		0.984	429.79	422.70
7-j	27.51	1	0.100	2	0.201	0.402	0.07	0.5	1.024	454.31	464.99
8-j	24.82	0	0	2	0.201	0.402	0.18	1.6	2.133	369.74	788.58
9-c	23.88	1	0.100	1	0.201	0.201	0.05	1.6	1.902	342.21	650.92
10-h	26.13	0	0	2	0.218	0.437	0.29		0.728	409.85	298.17
11-h	26.84	1	0.083	1	0.167	0.167	-0.12	0.9	1.001	432.39	432.93
12-i	27.02	1	0.100	1	0.201	0.201	0.07	0.5	0.822	438.31	360.33
13-i	25.238	0	0	2	0.201	0.402	0.48		0.883	382.17	337.38
14-p	23.76	0	0	2	0.12	0.24	-0.01	4.1	4.36	338.92	1477.70
15-o	26.92	0	0	1	0.12	0.12	0.31	2.6	3.03	435.10	1318.36
16-u	24.73	1	0.100	2	0.201	0.402	0.12	2.6	3.224	366.94	1182.84
17-x	25.46	1	0.109	2	0.218	0.437	0.29		0.837	389.14	325.66
18-x	23.98	1	0.083	2	0.167	0.335	-0.12	0.9	1.169	345.20	403.45
19-gg	25.63	1	0.109	2	0.218	0.437	0.29	0.5	1.287	394.20	507.29
20-gg	22.79	0	0	2	0.167	0.335	-0.12	1.6	1.765	311.63	550.03
21-hh	24.54	1	0.100	1	0.201	0.201	0.18	1.6	2.032	361.36	734.31
22-aa	27.42	0	0.109	1	0.218	0.218	0.1	0.6	0.881	451.21	397.63
23-z	25.23	1	0.083	1	0.167	0.167	-0.54	1.2	0.881	382.17	336.79
24-z	25.05	0	0.100	1	0.201	0.201	-0.01	0.6	0.811	376.50	305.49
25-dd	27.15	1	0.109	2	0.218	0.437	0.29		0.837	442.27	370.13
26-dd	27.63	0	0	2	0.167	0.335	-0.12	0.9	1.085	458.08	497.02
27-bb	26.14	1	0.109	2	0.218	0.437	0.29	0.5	1.287	410.23	527.92
28-bb	24.06	0	0	2	0.167	0.335	-0.12	1.6	1.765	347.45	613.24
29-cc	21.77	2	0.100	1	0.201	0.201	0.18	1.6	2.133	284.44	606.65
30-ee	26.63	1	0.109	1	0.218	0.218	-0.1	1.6	1.778	425.62	756.81
31-ff	27.26	0	0	3	0.167	0.502	-0.2	1.6	1.853	446.06	826.33
32-m	31.47	0	0	2	0.201	0.402	-3.52	5.1	1.988	594.33	1181.23
33-s	27.88	2	0.109	1	0.218	0.218	0.29		0.728	466.54	339.41
34-s	25.81	0	0	2	0.167	0.335	-0.12	0.9	1.085	399.82	433.80

Table 6.5: Dynamic loss in different ducts

Branch	V (m/s)	No.$_{45}$	K$_{45}$	No.$_{90}$	K$_{90}$	K$_b$	K$_a$	K$_d$	K	P$_v$	ΔP$_j$(Pa)
35-t	23.20	1	0.100	3	0.201	0.604	0.18	0.9	1.755	323.06	566.93
36-v	27.96	1	0.109	2	0.218	0.437	0.29		0.837	469.16	392.63
37-v	22.94	0	0	1	0.167	0.167	-0.12	1.6	1.598	315.88	504.62
38-y	26.70	1	0.109	2	0.218	0.437	0.29		0.837	428.02	358.20
39-y	25.13	1	0.083	2	0.167	0.335	-0.12	0.9	1.169	379.15	443.13
a-b	24.16	0	0	0	0	0	0.02	1.1	1.518	350.22	531.46
b-c	24.52	0	0	0	0	0	0.01		0.01	360.74	3.61
c-d	24.14	1	0.065	2	0.13	0.26	-0.14	0.1	0.249	349.64	86.99
e-d	27.96	0	0	0	0	0	0.31	0.9	1.255	469.06	588.67
d-f	26.01	0	0	0	0	0	0.05		0.05	405.91	20.30
h-f	27.68	1	0.079	2	0.159	0.318	-0.99	1.4	0.799	459.71	367.08
f-g	26.72	0	0	0	0	0	0	0	0	428.38	0.00
g-l	25.5	0	0	0	0	0	0.05	0.1	0.17	390.15	66.33
k-l	22.25	1	0.071	0	0	0	-0.99	1	0.07	297.04	20.79
j-k	24.2	0	0	0	0	0	0.07	0.9	0.94	351.38	330.30
l-p	25.65	0	0	0	0	0	0.3	0.1	0.36	394.75	142.11
p-q	23.62	0	0	1	0	0	-0.01		0.12	334.74	40.17
v-t	25.22	0	0	0	0	0	0.07		0.07	381.63	26.71
t-r	22.18	0	0	0	0	0	-0.01	1.6	1.54	295.17	454.56
r-n	22.86	1	0.062	0	0	0	0.02	0.4	0.48	313.55	150.50
n-m	23.86	0	0	0	0	0	0		0	341.58	0.00
u-n	22.85	0	0	0	0	0	0.48		0.48	313.27	150.37
w-u	22.78	2	0.065	1	0.13	0.13	-0.12	0.2	0.325	311.36	101.19
x-w	25.36	0	0	0	0	0	-0.12	1.7	1.62	385.88	625.12
y-w	26.67	0	0	0	0	0	0.29	1.1	1.35	426.77	576.14
dd-ee	28.65	0	0	0	0	0	0.1	0.5	0.55	492.49	270.87
ee-ff	23.02	1	0.071	0	0	0	-0.09	0.1	0.08	317.95	25.44
ff-kk	24.97	1	0.071	1	0.143	0.143	0.65	0.7	1.59	374.10	594.82
bb-cc	25.58	0	0	0	0	0	0.07		0.07	392.60	27.48
cc-ii	22.61	1	0.071	0	0	0	0.48	1.6	2.11	306.73	647.04
z-aa	23.66	0	0	0	0	0	-0.02	0	0	335.88	0.00
aa-jj	24.32	1	0.071	0	0	0	0.18	2.6	2.855	354.88	1013.18
gg-hh	24.48	0	0	0	0	0	0.07	0.2	0.238	359.56	85.40
hh-ii	22.12	2	0.071	0	0	0	0.02	1.6	1.714	293.58	503.13
ii-jj	22.18	0	0	0	0	0	0.07		0.07	295.17	20.66
jj-kk	23.23	0	0	0	0	0	-0.29	0.3	0	323.78	0.00
kk-20	23.09	1	0.06	2	0.12	0.24	-0.99	1	0.18	319.89	57.58
m-o	23.81	0	0.06	0	0	0	-0.01	0	0	340.15	0.00
i-g	23.4	1	0.079	1	0.159	0.159	0.11	0.8	1.139	328.54	374.20
o-q	24.6	0	0	0	0	0	0.3	0.2	0.48	363.10	174.29
s-r	27.51	1	0.079	0	0	0	0.3	0.9	1.25	454.08	567.37
q-20	24.75	1	0.06	0	0	0	0.05	0	0.12	367.54	44.10

A1.3 Safe thickness selection

The safe thickness of ducts is given in table 6.66.7

Table 6.6: Safe thickness selection

Branch	L (m)	Do (mm)	t (mm)	L/D0	D0/t	A	B	P_{am}	P_{as}	P_e	Comment
1-a	5	273.05	6.35	18.31166453	43	0.0006	57	1.76	1.70	0.1057	Safe
2-a	7	219.08	6.35	31.95179843	34.501	0.0009	64	2.47	2.45	0.1057	Safe
3-b	4.5	355.6	7.925	12.65466817	44.871	0.0005	54	1.60	1.60	0.1057	Safe
4-e	5.5	273.05	6.35	20.14283098	43	0.0006	57	1.76	1.70	0.1057	Safe
5-e	6	355.6	7.925	16.87289089	44.871	0.0005	54	1.60	1.60	0.1057	Safe
6-j	5	273.05	6.35	18.31166453	43	0.0006	57	1.76	1.70	0.1057	Safe
7-j	5	273.05	6.35	18.31166453	43	0.0006	57	1.76	1.70	0.1057	Safe
8-j	5	273.05	6.35	18.31166453	43	0.0006	57	1.76	1.70	0.1057	Safe
9-c	7.5	273.05	6.35	27.4674968	43	0.0006	60.5	1.87	1.85	0.1057	Safe
10-h	6	219.08	6.35	27.3872558	34.501	0.0009	84	3.24	3.25	0.1057	Safe
11-h	3	355.6	7.925	8.436445444	44.871	0.0005	56.5	1.67	1.60	0.1057	Safe
12-i	7	273.05	6.35	25.63633034	43	0.0006	57	1.76	1.70	0.1057	Safe
13-i	9	273.05	6.35	32.96099615	43	0.0006	57	1.76	1.70	0.1057	Safe
14-p	10	1219.2	8	8.202099738	152.4	0.00007	7.2	0.05	0.05	0.1057	Unsafe
15-o	5	812.8	8	6.151574803	101.6	0.00018	17.9	0.23	0.20	0.1057	Safe
16-u	5	273.05	6.35	18.31166453	43	0.0006	57	1.76	1.70	0.1057	Safe
17-x	5	219.08	6.35	22.82271316	34.501	0.009	64	2.47	2.45	0.1057	Safe
18-x	5	355.6	7.925	14.06074241	44.871	0.0005	54	1.60	1.60	0.1057	Safe
19-gg	5	219.08	6.35	22.82271316	34.501	0.009	64	2.47	2.40	0.1057	Safe
20-gg	5	355.6	7.925	14.06074241	44.871	0.0005	54	1.60	1.60	0.1057	Safe
21-hh	5	273.05	6.35	18.31166453	43	0.0006	57	1.76	1.70	0.1057	Safe
22-aa	5	219.08	6.35	22.82271316	34.501	0.009	64	2.47	2.45	0.1057	Safe
23-z	5	355.6	7.925	14.06074241	44.871	0.0005	54	1.60	1.60	0.1057	Safe
24-z	5	273.05	6.35	18.31166453	43	0.0006	57	1.76	1.70	0.1057	Safe
25-dd	6	219.08	6.35	27.3872558	34.501	0.0009	84	3.24	3.25	0.1057	Safe
26-dd	4	355.6	7.925	11.24859393	44.871	0.0004	40	0.11	0.11	0.1057	Safe
27-bb	5	219.08	6.35	22.82271316	34.501	0.009	64	2.47	2.45	0.1057	Safe
28-bb	5	355.6	7.925	14.06074241	44.871	0.0005	54	1.60	1.60	0.1057	Safe
29-cc	8	273.05	6.35	29.29866325	43	0.00005	1.2	0.108	0.108	0.1057	Safe
30-ee	3	219.08	6.35	13.6936279	34.501	0.0009	64	2.47	2.45	0.1057	Safe
31-ff	5	355.6	7.925	14.06074241	44.871	0.0005	54	1.60	1.60	0.1057	Safe
32-m	5	273.05	6.35	18.31166453	43	0.0006	57	1.76	1.70	0.1057	Safe
33-s	5	219.08	6.35	22.82271316	34.501	0.009	64	2.47	2.45	0.1057	Safe
34-s	5	355.6	7.925	14.06074241	44.871	0.0005	54	1.60	1.60	0.1057	Safe

Table 6.7: Safe thickness selection

Branch	L (m)	Do (mm)	t (mm)	L/D0	D0/t	A	B	P_{am}	P_{as}	P_e	Comment
35-t	5	273.05	6.35	18.31166453	43	0.0006	57	1.76	1.70	0.1057	Safe
36-v	5	219.08	6.35	22.82271316	34.501	0.009	64	2.47	2.45	0.1057	Safe
37-v	5	355.6	7.925	14.06074241	44.871	0.0005	54	1.60	1.60	0.1057	Safe
38-y	5	219.08	6.35	22.82271316	34.501	0.009	64	2.47	2.45	0.1057	Safe
39-y	5	355.6	7.925	14.06074241	44.871	0.0005	54	1.60	1.60	0.1057	Safe
a-b	1	355.6	7.925	2.812148481	44.871	0.001	70	2.08	2.00	0.1057	Safe
b-c	1.5	508	6.35	2.952755906	80	0.0005	56	0.93	0.95	0.1057	Safe
c-d	6.5	609.6	8	10.66272966	76.2	0.0002	20.06	0.35	0.35	0.1057	Safe
e-d	6	457.2	7.925	13.12335958	57.691	0.0003	32	0.73	0.75	0.1057	Safe
d-f	5	711.2	8	7.030371204	88.9	0.00019	19	0.28	0.28	0.1057	Safe
h-f	7.5	406.4	7.925	18.45472441	51.281	0.0004	40.9	1.06	1.00	0.1057	Safe
f-g	1	812.8	8	1.230314961	101.6	0.0015	65.5	0.85	0.88	0.1057	Safe
g-l	12	863.6	8	13.89532191	107.95	0.00009	8.9	0.10	0.10	0.1057	Safe
k-l	5	508	6.35	9.842519685	80	0.0001	18	0.30	0.30	0.1057	Safe
j-k	5	406.4	7.925	12.30314961	51.281	0.0004	41	1.06	1.00	0.1057	Safe
l-p	60	1016	8	59.05511811	127	0.00006	6.5	0.06	0.05	0.1057	Unsafe
p-q	5	1616	8	3.094059406	202	0.0001	13	0.08	0.008	0.1057	Unsafe
v-t	5	406.4	7.925	12.30314961	51.281	0.0004	41	1.06	1.00	0.1057	Safe
t-r	5	508	6.35	9.842519685	80	0.0002	28	0.46	0.50	0.1057	Safe
r-n	5	660.4	8	7.571168988	82.55	0.0002	28	0.45	0.45	0.1057	Safe
n-m	5	863.6	8	5.789717462	107.95	0.0001	17	0.20	0.20	0.1057	Safe
u-n	5	660.4	8	7.571168988	82.55	0.0002	20	0.32	0.31	0.1057	Safe
w-u	5	609.6	9.33	8.202099738	65.338	0.0002	28	0.57	0.55	0.1057	Safe
x-w	5	406.4	7.925	12.30314961	51.281	0.0004	41	1.06	1.00	0.1057	Safe
y-w	5	406.4	7.925	12.30314961	51.281	0.0004	41	1.06	1.00	0.1057	Safe
dd-ee	1	406.4	7.925	2.460629921	51.281	0.0013	69.62	1.81	1.80	0.1057	Safe
ee-ff	4	508	9.525	7.874015748	53.333	0.0004	41	1.02	1.00	0.1057	Safe
ff-kk	5	508	9.33	9.842519685	54.448	0.0002	28.5	0.69	0.70	0.1057	Safe
bb-cc	3	406.4	7.925	7.381889764	51.281	0.0004	45.6	1.18	1.20	0.1057	Safe
cc-ii	5	508	9.525	9.842519685	53.333	0.0004	39.5	0.98	0.99	0.1057	Safe
z-aa	5	508	7.925	9.842519685	64.101	0.0003	33	0.68	0.70	0.1057	Safe
aa-jj	5	508	9.525	9.842519685	53.333	0.0004	39.5	0.98	0.99	0.1057	Safe
gg-hh	12	406.4	7.925	29.52755906	51.281	0.0004	40.5	1.05	1.00	0.1057	Safe
hh-ii	11	508	6.35	21.65354331	80	0.0001	12	0.20	0.20	0.1057	Safe
ii-jj	9	711.2	8	12.65466817	88.9	0.0001	14.2	0.21	0.20	0.1057	Safe
jj-kk	5	863.6	8	5.789717462	107.95	0.0001	17.5	0.21	0.20	0.1057	Safe
kk-20	16	1117.6	8	14.31639227	139.7	0.00009	6.34	0.16	0.15	0.1057	Unsafe
m-o	5	966	8	5.175983437	120.75	0.0001	17	0.18	0.20	0.1057	Safe
i-g	5	406.4	7.925	12.30314961	51.281	0.0003	32	0.83	0.83	0.1057	Safe
o-q	5	1266	8	3.949447077	158.25	0.0001	15	0.12	0.11	0.1057	Safe
s-r	5	406.4	7.925	12.30314961	51.281	0.0004	41	1.07	1.00	0.1057	Safe
q-20	25	2016	8	12.40079365	252	0.000022	2	0.01	0.01	0.1057	Unsafe

A1.4 Maximum span selection

The calculation of maximum safe span is calculated and given in table 6.86.9

Table 6.8: Maximum safe span selection

Branch	D(mm)	L (m)	Schedule	OD(mm)	t(mm)	ID(mm)	L_{max}
1-a	250	5	20	273.05	6.35	260.35	3.280
2-a	200	7	20	219.08	6.35	206.38	2.980
3-b	350	4.5	20	355.6	7.925	339.75	3.740
4-e	250	5.5	20	273.05	6.35	260.35	3.280
5-e	350	6	20	355.6	7.925	339.75	3.740
6-j	250	5	20	273.05	6.35	260.35	3.280
7-j	250	5	20	273.05	6.35	260.35	3.280
8-j	250	5	20	273.05	6.35	260.35	3.280
9-c	250	7.5	20	273.05	6.35	260.35	3.280
10-h	200	6	20	219.08	6.35	206.38	2.980
11-h	350	3	20	355.6	7.925	339.75	3.740
12-i	250	7	20	273.05	6.35	260.35	3.280
13-i	250	9	20	273.05	6.35	260.35	3.280
14-p	1200	10	MANUFACTURED	1216	8	1200	6.070
15-o	800	5	MANUFACTURED	803.6	8	787.6	5.220
16-u	250	5	20	273.05	6.35	260.35	3.280
17-x	200	5	20	219.08	6.35	206.38	2.980
18-x	350	5	20	355.6	7.925	339.75	3.740
19-gg	200	5	20	219.08	6.35	206.38	2.980
20-gg	350	5	20	355.6	7.925	339.75	3.740
21-hh	250	5	20	273.05	6.35	260.35	3.280
22-aa	200	5	20	219.08	6.35	206.38	2.980
23-z	350	5	20	355.6	7.925	339.75	3.740
24-z	250	5	20	273.05	6.35	260.35	3.280
25-dd	200	6	20	219.08	6.35	206.38	2.980
26-dd	350	4	20	355.6	7.925	339.75	3.740
27-bb	200	5	20	219.08	6.35	206.38	2.980
28-bb	350	5	20	355.6	7.925	339.75	3.740
29-cc	250	8	20	273.05	6.35	260.35	3.280
30-ee	200	3	20	219.08	6.35	206.38	2.980
31-ff	350	5	20	355.6	7.925	339.75	3.740
32-m	250	5	20	273.05	6.35	260.35	3.280
33-s	200	5	20	219.08	6.35	206.38	2.980
34-s	350	5	20	355.6	7.925	339.75	3.740

Table 6.9: Maximum safe span selection

Branch	D(mm)	L (m)	Schedule	OD(mm)	t(mm)	ID(mm)	L_{max}
35-t	250	5	20	273.05	6.35	260.35	3.280
36-v	200	5	20	219.08	6.35	206.38	2.980
37-v	350	5	20	355.6	7.925	339.75	3.740
38-y	200	5	20	219.08	6.35	206.38	2.980
39-y	350	5	20	355.6	7.925	339.75	3.740
a-b	350	1	20	355.6	7.925	339.75	3.740
b-c	500	1.5	10	508	6.35	495.3	4.250
c-d	600	6.5	MANUFACTURED	606.94	8	590.94	4.670
e-d	450	6	20	457.2	7.925	441.35	4.160
d-f	700	5	MANUFACTURED	704.6	8	688.6	4.960
h-f	400	7.5	20	406.4	7.925	390.55	3.960
f-g	800	1	MANUFACTURED	803.6	8	787.6	5.220
g-l	900	12	MANUFACTURED	905.6	8	889.6	3.960
k-l	500	5	10	508	6.35	495.3	5.460
j-k	400	5	20	406.4	7.925	390.55	4.250
l-p	1000	60	MANUFACTURED	1016	8	1000	3.960
p-q	1600	5	MANUFACTURED	1616	8	1600	5.690
v-t	400	5	20	406.4	7.925	390.55	6.700
t-r	500	5	10	508	6.35	495.3	3.960
r-n	600	5	MANUFACTURED	666	8	650	4.250
n-m	900	5	MANUFACTURED	916	8	900	4.850
u-n	650	5	MANUFACTURED	666	8	650	5.480
w-u	600	5	MANUFACTURED	609.6	9.33	590.94	4.850
x-w	400	5	20	406.4	7.925	390.55	4.750
y-w	400	5	20	406.4	7.925	390.55	3.960
dd-ee	400	1	20	406.4	7.925	390.55	3.960
ee-ff	500	4	20	508	9.525	488.95	3.960
ff-kk	600	5	20	609.6	9.33	590.94	4.410
bb-cc	400	3	20	406.4	7.925	390.55	4.750
cc-ii	500	5	20	508	9.525	488.95	3.960
z-aa	450	5	20	457.2	7.925	441.16	4.410
aa-jj	500	5	20	508	9.525	488.95	4.160
gg-hh	400	12	20	406.4	7.925	390.55	4.410
hh-ii	500	11	10	508	6.35	495.3	3.960
ii-jj	700	9	MANUFACTURED	716	8	700	4.250
jj-kk	900	5	MANUFACTURED	864	8	848	4.990
kk-20	1100	16	MANUFACTURED	1066	8	1050	5.360
m-o	950	5	MANUFACTURED	966	8	950	5.790
i-g	400	5	20	406.4	7.925	390.55	5.590
o-q	1250	5	MANUFACTURED	1266	8	1250	3.960
s-r	400	5	20	406.4	7.925	390.55	6.160
q-20	2000	25	MANUFACTURED	2016	8	2000	7.210